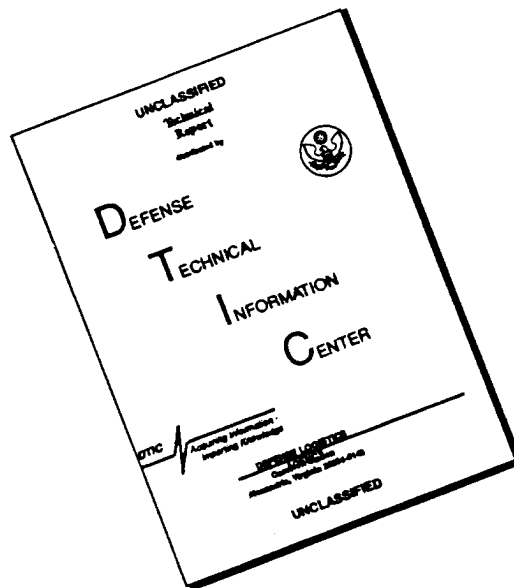


REPORT DOCUMENTATION PAGE			Form Approved OMB No. 0704-0188	
<small>Public reporting burden for this collection of information is estimated to average 1 hour per response, including the time for reviewing instructions, searching existing data sources, gathering and maintaining the data needed, and completing and reviewing the collection of information. Send comments regarding this burden estimate or any other aspect of this collection of information, including suggestions for reducing this burden, to Washington Headquarters Services, Directorate for Information Operations and Reports, 1215 Jefferson Davis Highway, Suite 1204, Arlington, VA 22202-4302, and to the Office of Management and Budget, Paperwork Reduction Project (0704-0188), Washington, DC 20503.</small>				
1. AGENCY USE ONLY (Leave blank)	2. REPORT DATE 8/16/96	3. REPORT TYPE AND DATES COVERED Final Technical Report 7/1/94 to 6/30/96		
4. TITLE AND SUBTITLE Monte Carlo Analysis of Nonequilibrium Ionized Flows			5. FUNDING NUMBERS PE - 61102F PR - 2308 SA - AS G - F49620-94-1-0328	
6. AUTHOR(S) Iain D. Boyd				
7. PERFORMING ORGANIZATION NAME(S) AND ADDRESS(ES) Cornell University 246 Upson Hall Ithaca, NY 14853			AFOSR-TR-96 0449	
9. SPONSORING / MONITORING AGENCY NAME(S) AND ADDRESS(ES) AFOSR/NA 110 Duncan Avenue, Suite B115 Bolling AFB, DC 20332-0001			10. SPONSORING MONITORING AGENCY REPORT NUMBER NA 94-1-0328	
11. SUPPLEMENTARY NOTES				
12a. DISTRIBUTION / AVAILABILITY STATEMENT Approved for public release; distribution is unlimited			12b. DISTRIBUTION CODE	
13. ABSTRACT (Maximum 200 words) This final report summarizes the research carried out by our research group concerned with the development of a numerical approach for simulating the flows through and expanding from low-power hydrogen arcjets. In Section I, we describe the development of a particle-based Monte Carlo approach for simulating the necessary collision and plasma effects that occur in these electric propulsion devices. In Section II, we describe an extensive study to make comparison between our model predictions and existing experimental data. It is concluded that the Monte Carlo approach provides an accurate means for simulating the flow inside of the nozzle of the arcjet offering the potential to improve arcjet performance. It is also concluded that accurate Monte Carlo simulation of the arcjet plumes offers the potential to assess accurately integration of arcjets with real spacecraft geometries.				
14. SUBJECT TERMS Arcjet (electric) propulsion; Numerical Simulation			15. NUMBER OF PAGES 43	
			16. PRICE CODE	
17. SECURITY CLASSIFICATION OF REPORT	18. SECURITY CLASSIFICATION OF THIS PAGE	19. SECURITY CLASSIFICATION OF ABSTRACT	20. LIMITATION OF ABSTRACT	

DISCLAIMER NOTICE



THIS DOCUMENT IS BEST QUALITY AVAILABLE. THE COPY FURNISHED TO DTIC CONTAINED A SIGNIFICANT NUMBER OF PAGES WHICH DO NOT REPRODUCE LEGIBLY.

FINAL TECHNICAL REPORT

For research supported by
AFOSR Contract No. F49620-94-1-0328 (Year 2)

for the period 07/01/94 to 06/30/96

MONTE CARLO ANALYSIS OF NONEQUILIBRIUM IONIZED FLOWS

prepared by

Iain D. Boyd (1)
Xiaoming Liu (2) and Jitendra Balakrishnan (2)

School of Mechanical and Aerospace Engineering
Cornell University,
246 Upson Hall
Ithaca, NY 14853.

Work supported by

Air Force Office of Scientific Research
Program Manager: Dr. Mitat A. Birkan

August 1996

(1) Principal Investigator

(2) Graduate Research Assistant

19961015 013

Table of Contents

	Page
Abstract	3
Overview	4
I. Monte Carlo Model of Hydrogen Arcjet Flows	5
II. Extensive Validation of the Monte Carlo Model	24

Abstract

This final report summarizes the research carried out by our research group concerned with the development of a numerical approach for simulating the flows through and expanding from low-power hydrogen arcjets. In Section I, we describe the development of a particle-based Monte Carlo approach for simulating the necessary collision and plasma effects that occur in these electric propulsion devices. In Section II, we describe an extensive study to make comparison between our model predictions and existing experimental data. It is concluded that the Monte Carlo approach provides an accurate means for simulating the flow inside of the nozzle of the arcjet offering the potential to improve arcjet performance. It is also concluded that accurate Monte Carlo simulation of the arcjet plumes offers the potential to assess accurately integration of arcjets with real spacecraft geometries.

Overview

Arcjets are being installed on spacecraft for a variety of orbit maintenance tasks. There is a requirement for development of physically accurate numerical models to describe the nozzle and plume flows of these thrusters. Accurate simulation of nozzle flows offers the potential to use the model to optimize the flow conditions and geometry of the arcjet to improve propulsion efficiency which is usually of the order of 30-40%. This is particularly important as the need for small-scale thrusters becomes an important component in the development of micro- and nano-satellites. Accurate simulation of arcjet plumes is necessary for prediction of spacecraft interaction effects such as contamination of solar arrays, torques, and surface heating.

The modeling effort reported here has led to the development of a Monte Carlo model for describing the nozzle and plume flows of a 1 kW arcjet. This work focused on the flow of hydrogen through the arcjet due to the availability of a large volume of detailed experimental data for this configuration. Development of the Monte Carlo model required implementation of high-temperature kinetics and plasma models for the hydrogen system. This work is described in Section I. The Monte Carlo approach offers the possibility of simulating nonequilibrium transport and chemical kinetics effects compared to continuum formulations. In addition, direct simulation of the important plasma effect of ohmic heating is included in the Monte Carlo technique for the first time. The inclusion of ohmic heating is required to predict the specific impulse measured experimentally. This work was presented as an invited paper (AIAA 96-2022) at the AIAA 27th Fluid Dynamics Conference, New Orleans, Louisiana, June 1996.

An extensive series of comparisons between the Monte Carlo predictions and detailed experimental data was conducted in: (1) the interior nozzle flow; (2) the nozzle exit plane; and (3) the arcjet plume. The comparisons of properties in the arcjet plume are the first of their kind. Continuum numerical methods are generally unable to compute the plume flows due to their very low density. These comparisons are described in Section II. Generally, very good agreement between computations and measurements was obtained for flow properties such as number densities, velocities, and temperatures for the interior nozzle flow, for the nozzle exit plane, and for the plume expansion. Good agreement was also obtained with measurements of specific impulse. The only flow field property for which there was significant disagreement was the number density of atomic hydrogen which was consistently predicted to be a factor of 3 to 4 lower than values measured experimentally at the Phillips Laboratory. This work was presented as a contributed paper (AIAA 96-3297) at the 32nd AIAA/ASME/SAE/ASEE Joint Propulsion Conference, Orlando, Florida, July 1996. An additional paper presented at this conference (Wysong, Pobst and Boyd, "Comparisons of Hydrogen Atom Measurements in an Arcjet Plume With DSMC Predictions," AIAA Paper 96-3185) also resulted from this research effort.

The conclusion drawn from these studies is that the Monte Carlo approach is an appropriate method for accurate modeling of the nozzle and plume flows of hydrogen arcjets. The arcjets manufactured by Olin Aerospace that are being flown in space use hydrazine as propellant. To model the flows of the real thrusters, extension of the Monte Carlo model is required to include the more complicated kinetics mechanisms of the H₂-N₂ system.

I. MONTE CARLO MODEL OF HYDROGEN ARCJET FLOWS

Abstract

A particle-based Monte Carlo numerical method is developed for computation of flow in a low-thrust hydrogen arcjet. The method employs the direct simulation Monte Carlo technique to compute the nonequilibrium fluid mechanics and thermochemical relaxation. Simulation of plasma effects is included at a simple level that ensures charge neutrality. A new model is developed to include ohmic heating in the simulation. Results are presented for a flow condition that has been studied experimentally with a number of different diagnostic techniques. A strong degree of thermal nonequilibrium is found in the flow. It is demonstrated that ohmic heating is important, and that the Monte Carlo model captures the important physics very well. It is also found that the simple model employed for motion of the charged species is inadequate leading to poor prediction of some flow properties.

Introduction

Arcjets operated at a power level of about 1 kW are an attractive candidate for use as electric propulsion devices on spacecraft. They offer substantial increases in specific impulse compared with chemical rockets and resistojets. Unfortunately, the performance of arcjets remains poor with propulsion efficiencies in the range of 30 to 50%. There is a need for accurate numerical simulation of the flows generated by these devices both for improving their performance, and for analysis of potential spacecraft interaction effects such as contamination. There are many coupled physical phenomena at work in an arcjet that makes numerical simulation difficult. Nonequilibrium kinetic processes include rotational and vibrational relaxation, and several chemical mechanisms including dissociation, recombination, and ionization. In addition plasma effects are important.

A hydrazine arcjet has been developed and flown in space.¹ In terms of basic research, however, hydrogen arcjets have received considerable attention. Several experimental studies have been conducted on an arc-jet designed and fabricated at NASA Lewis Research Center. A schematic diagram of this thruster is shown in Fig. 1. The NASA Lewis hydrogen arcjet has been used in experimental investigations to determine its performance² and flow fields.³⁻⁴ Of considerable importance is the fact that several different diagnostic techniques have been applied to these flows yielding measurements that include translational and rotational temperature, velocity, and number densities of atomic and molecular hydrogen. These data offer excellent opportunities for detailed calibration of modeling efforts. Arcjet models based on continuum formulations have been developed by several groups.⁵⁻⁸ There are two main problems with the continuum approach. First, there is a significant degree of thermal and chemical nonequilibrium in these flows. Second, it is very difficult to extend the continuum simulations out to the plume produced by the arcjet. This means that these methods cannot be used to predict spacecraft interference effects.

This paper describes the development of the direct simulation Monte Carlo method (DSMC) for application to a hydrogen arcjet. In satellite propulsion, the DSMC technique has been applied and successfully

verified to the plume of a hydrazine rocket⁹, and to the nozzle and plume flows of both a nitrogen resisto-jet¹⁰ and a cold flow of hydrogen through an arcjet.¹¹ Preliminary DSMC results for heated arcjet flows were reported in Ref. 5. In this paper, description is provided of the collision and chemistry models developed for this application. In addition, the implementation of plasma effects are discussed. In particular, this study describes a new model for computation of ohmic heating using the DSMC technique. Results are presented to illustrate the general nonequilibrium nature of the arcjet flows and comparison is made with experimental data.

Numerical Method

The direct simulation Monte Carlo method (DSMC) uses the motions and collisions of particles to perform a direct simulation of nonequilibrium gas dynamics. Each particle has coordinates in physical space, three velocity components, and internal energies. A computational grid is employed to group together particles that are likely to collide. Collision selection is based on a probability model developed from basic concepts in kinetic theory. The method is widely used for rarefied nonequilibrium conditions and finds application in hypersonics, materials processing, and micro-machine flows.

The extension of the technique for application to arcjet flows requires development of a number of new physical models. Arcjets are characterized by high temperatures (as high as 30,000 K) which give rise to strongly ionized flows (as much as 30% ionized). In terms of intermolecular collisions, mechanisms must be included in the numerical model to account for: (1) momentum transfer; (2) rotational excitation; (3) vibrational excitation; (4) dissociation/recombination; and (5) ionization/recombination. The relatively high level of ionization requires modeling of plasma effects at some level. Each of these modeling issues is discussed in the following.

Momentum Transfer

For a hydrogen arcjet, the four main species present are H_2 , H , H^+ , and e^- . In general, the most important collision types that determine the arcjet flow field are H_2-H_2 , H_2-H , $H-H$, H_2-e^- , and $H-e^-$. In the present work, the momentum transfer cross-sections for the first three collision types are obtained from the work of Vanderslice et al.¹² in which collision integrals were tabulated for the temperature range of 1,000 to 15,000 K. These collision integrals are first converted into total collision cross sections and are shown in Fig. 2. Using this data, appropriate parameters are determined for the Variable Hard Sphere (VHS) collision model¹³ that is widely used in DSMC computations. In the present DSMC code, a single value of the viscosity temperature exponent ω that appears in the VHS model is used for all collision types. This places a small restriction on the level of agreement that is achievable for all collisions. The VHS parameters identified as providing the best fit to the data are: $\omega=0.82$, $T_{ref}=300$ K, with reference collision cross-sections of $\sigma_{H_2-H_2}=3.554 \times 10^{-19}$ m², $\sigma_{H_2-H}=3.140 \times 10^{-19}$ m², and $\sigma_{H-H}=3.554 \times 10^{-19}$ m². Comparison of the VHS models to the data of Ref. 12 is made in Fig. 2. The viscosities obtained using these VHS parameters are compared with the computations of Vanderslice et al. as a function of temperature in Fig. 3. The level of

agreement is quite good. Also shown in Fig. 3 is the viscosity obtained when VHS parameters for hydrogen for low temperature flows are employed. In this case, the VHS parameters are: $\omega=0.67$, $T_{ref}=273$ K, $\sigma_{H_2-H_2} = \sigma_{H_2-H} = \sigma_{H-H} = 2.606 \times 10^{-19}$ m². These parameters were used in the previous study that applied the DSMC technique to cold hydrogen flow through an arcjet geometry.¹¹ These results provide an indication of the sensitivity of the flow field modeling to momentum transfer.

The VHS reference cross-section for the H_2-e^- collision is determined to be $\sigma_{H_2-e^-}=3.547 \times 10^{-19}$ m² using the experimental data of Crompton and Sutton.¹⁴ Comparison of the model and the data is shown in Fig. 4. The range of relative velocity computed for the VHS model corresponds to the thermal speed of electrons over the temperature range from 1,000 to 15,000 K. Clearly, the VHS model does not capture the data very well. This represents a requirement for further development in the future. The VHS reference cross-section for the $H-e^-$ collision is determined to be $\sigma_{H-e^-}=7.118 \times 10^{-19}$ m² using the simple analytical expression given by Yos.¹⁵ Comparison of the VHS model with this expression is shown in Fig. 5 and reveals generally very good agreement except at very low temperatures.

Other cross-sections are much less important and are assigned values such that the results of hydrogen atoms are used for hydrogen ions. For example, the cross-sections shown in Fig. 2 for H_2-H collisions are also used for H_2-H^+ collisions. While this results in some lack of accuracy, it is expected that the effect will be small as these collisions are relatively infrequent.

Rotational and Vibrational Relaxation

Molecular hydrogen is an interesting diatomic molecule in that it has relatively large values for the characteristic temperatures of rotation and vibration. This results in long relaxation times for these modes. In the present work, the transfer of energy between the translational and rotational energy modes employs the phenomenological approach of Borgnakke-Larsen.¹⁶ In this scheme, a probability of exchanging energy is applied to each collision. If it is decided that energy transfer does occur, the post-collision energies are sampled from equilibrium energy distributions. Previously, a probability model for determining the probability of translational-rotational energy transfer for hydrogen at low temperatures was developed and verified.¹¹ This same model is employed again here although it is recognized that it may be inaccurate at the very high temperatures encountered in the arcjet.

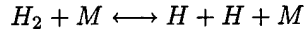
Vibrational energy is modeled using the quantized oscillator form of the Borgnakke-Larsen approach developed by Boyd and Bergemann.¹⁷ The probability of vibrational energy exchange employs the familiar Landau-Teller relaxation time with parameters obtained experimentally by Kiefer.¹⁸ Once again it is recognized that this approach may be inaccurate at the very high temperatures found in the arcjet.

The average probabilities of rotational (RT) and vibrational (VT) energy exchange for H_2-H_2 collisions are compared as a function of temperature in Fig. 6.

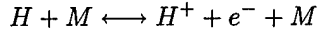
Chemical Reactions

There are only two chemical reactions implemented in the present study. They are dissociation of

molecular hydrogen:



and ionization of atomic hydrogen:



where in each case M is any available species. The dissociation rate for $M=H_2$, H , and H^+ is obtained from Ref. 19 as $1.82 \times 10^{-14} T^{-0.251} \exp(-51,275/T) \text{ m}^3/\text{sec}$. For dissociation through electron impact, the rate is taken from McCay and Dexter²⁰ as $3.17 \times 10^{-19} T^{1.0} \exp(-51,275/T) \text{ m}^3/\text{sec}$. The ionization rate for $M=H_2$, H , and H^+ is taken from Ref. 20 as $7.00 \times 10^{-12} T^{-1.0} \exp(-157,825/T) \text{ m}^3/\text{sec}$. For electron impact ionization, Ref. 20 gives the rate as $5.27 \times 10^1 T^{-3.0} \exp(-157,825/T) \text{ m}^3/\text{sec}$. It is not possible to capture this temperature dependence using the standard DSMC chemistry model. In particular, the temperature exponent for this collision pair must be no smaller than about -1. An expression that provides reasonable agreement with the actual rate is $1.32 \times 10^{-8} T^{-1.0} \exp(-120,000/T) \text{ m}^3/\text{sec}$. Comparison of the exact rate and the expression used in the DSMC computation is shown in Fig. 7.

The dissociation and ionization reactions are modeled using the DSMC chemistry model developed by Boyd.²¹ In the case of dissociation, the coupling to the vibrational energy is set to zero. Recombination reaction rates are computed from the above forward rates and the equilibrium constants. These reactions are then simulated using the DSMC recombination model described in Ref. 21.

Plasma Modeling

In principle, it is possible to model plasma effects using the particles of the DSMC algorithm through the addition of Particle In Cell (PIC)²² steps into the computer code. In practise, there is such a large discrepancy between the plasma and the collision length scales that need to be resolved in the arcjet flow, that this approach is infeasible. Instead, a very simple scheme is employed in which the electrons are constrained to move through the flow field with the average ion velocity in each cell. This ensures charge neutrality, but obviously omits the charge field effects.

A second important plasma effect that is included in the DSMC simulation is ohmic heating. This is an important source of energy that results from the current represented by the flux of charged species through the thruster. The electrical resistivity is given by:

$$\eta = \frac{m_e \sum_i \nu_{ei}}{n_e e^2} \quad (1)$$

where e is the charge of an electron, m_e is the electron mass, n_e is the electron number density, and ν_{ei} is the mean collision rate between an electron and heavy particle i . Power generated in the plasma due to ohmic heating is:

$$\Omega = \eta J^2. \quad (2)$$

Here, \mathbf{J} is the current vector so that

$$J^2 = e^2[(n_i u_i - n_e u_e)^2 + (n_i v_i - n_e v_e)^2] \quad (3)$$

where n_i is the ion number density, u_i and v_i are the mean ion velocities in the z and r directions, and u_e and v_e are the mean electron velocities in the z and r directions. The mean collision rates required by Eq. (1) for e^- - H_2 and e^- - H interactions are computed directly in the DSMC simulation. For the purposes of ohmic heating, a more accurate value of the e^- - H^+ interaction is computed using the Coulombic cross-section:

$$\langle \sigma_{e^- - H^+} \rangle = \frac{e^4}{24\pi(\epsilon_o k T_e)^2} \log(\Lambda) \quad (4)$$

where ϵ_o is the permittivity of free space, T_e is the electron temperature, and

$$\Lambda = \frac{12\pi(\epsilon_o k T_e)^{\frac{3}{2}}}{e^3 n_e^{\frac{1}{2}}}. \quad (5)$$

The total ohmic power is calculated in each cell of the simulation using Eqs. (1-5). The energy represented by Ω is added to the thermal energies of the charged species (electrons and ions) in each cell. The average energy to be added to each charged particle in the cell per time-step is then given by:

$$E = \frac{\Omega \Delta t}{n \Delta V} \quad (6)$$

where Δt is the simulation time step, ΔV is the cell volume, and n is the total number density of charged particles. The energy addition is performed such that momentum is conserved on average. This is achieved by increasing only the thermal velocity components of each charged particle by an amount proportional to \sqrt{E} .

Simulation Details

The collision and plasma models are implemented in an existing DSMC code that is designed for efficient performance on vector supercomputers.²³ Modest changes have also been made to allow the code to execute efficiently on work-stations. The addition of the ohmic heating model adds only a 20% overhead to the performance of the DSMC code.

The DSMC computations are begun at a location downstream of the nozzle throat. The initial profiles of flow properties are obtained from continuum simulations provided by the code of Butler.⁵ The interaction of the gas with the wall of the nozzle is assumed to be diffuse with full energy accommodation to the wall temperature profile obtained from the continuum simulation. Charged species are neutralized upon contact with the wall. The computations extend through the nozzle exit plane to a distance of 30 mm from the thruster along the axis. Expansion is assumed to occur into a perfect vacuum.

The grids employed typically consist of 500 by 55 cells. Due to the wide dynamic range in density for these flows, the cells are adapted to the local mean free path, and the time step in each cell is scaled by the local mean time between collisions. Despite the time step variation, the transient phase of the simulation

remains long. Typically, it requires at least 15,000 iterations before steady state is reached. Macroscopic results are then obtained by sampling properties over a further 10,000 time steps. At steady state, there are at least 300,000 particles present in the simulation.

Results

In terms of results, this investigation focuses on some of the nonequilibrium aspects of hydrogen arcjet flows. More detailed comparisons of experimental data with results obtained using the DSMC code described in this paper are reported in Refs. 24-25. The case considered here is for a power level of $P=1.4$ kW, and a mass flow rate, $\dot{m}=13.3$ mg/sec. These are conditions that have been investigated experimentally in a series of investigations by Cappelli and his co-workers at Stanford University, and at the Phillips Laboratory. First, results are presented that are obtained using the cross-sections of Vanderslice et al.. Next, the effect of the ohmic heating model is assessed. Finally, sensitivity of the solutions to changing the cross-sections for neutral interactions is considered.

Standard Computation

The following results are obtained using the collision and plasma models described earlier. In Fig. 8a, the concentrations of molecular and atomic hydrogen across the nozzle exit plane are shown. Experimental measurement of H_2 was performed by Beattie and Cappelli²⁶ using Raman scattering. The measurements for H are those reported by Wysong et al..²⁴ In general, the agreement between computation and measurement is better for H_2 than for H. In particular, the simulations predict an atomic concentration on the axis that is a factor of 3 to 4 smaller than the experimental data.

In Fig. 8b, the translational temperature profile of atomic hydrogen across the nozzle exit plane is shown. Two sets of experimental data reported by Wysong et al.²⁴ and by Storm and Cappelli²⁷ are shown. In general, the DSMC results show a small underprediction of the temperature, although the agreement is quite good. The degree of thermal nonequilibrium of the flow in the nozzle exit is illustrated in Fig. 8c. Here, the translational, rotational, and vibrational temperatures of molecular hydrogen predicted by the DSMC technique are compared with the rotational temperature measurements of Beattie and Cappelli.²⁶ The predicted rotational temperatures offer satisfactory agreement with the measured data. The peak vibrational temperature is about a factor of two higher than the peak translational temperature.

A further indication of the degree of thermal nonequilibrium in this flow is illustrated in Fig. 8d in which the electron temperature in the nozzle exit plane is shown. The experimental data is due to Storm and Cappelli.²⁸ The DSMC results show a relatively high degree of statistical scatter due to the small number of particles in the simulation that represent the electrons. Nevertheless, it is clear that the behavior close to the axis is very well captured by the simulation. Note that the peak electron temperature is an order of magnitude higher than the peak translational temperature. In Fig. 8e, the electron concentration across the nozzle exit plane is shown. The experimental data was also reported in Ref. 28. The agreement between simulation and measurement is very poor with the DSMC technique predicting concentrations that are an

order of magnitude higher than the data.

Finally, the axial component of velocity in the nozzle exit plane is shown in Fig. 8f. The experimental data is that of Wysong et al.²⁴ The DSMC results are consistently lower than the measured data across the entire exit plane. In Fig. 8g, the axial velocity along the nozzle centerline is shown. The experimental data is that of Storm and Cappelli.²⁹ Note that these data were taken at a slightly higher arcjet power of $P=1.48$ kW. It is evident that the DSMC simulation predicts lower velocities than the measured data along the entire extent of the nozzle. It should also be noted that the specific impulse predicted by the DSMC code is 780 sec in comparison to a value of about 900 measured at NASA Lewis Research Center under similar conditions.²

Effect of Ohmic Heating

A second simulation is performed in which the ohmic heating model is not employed in the DSMC computation. It is found that the absence of ohmic heating most affects the temperatures in the computed flow field. In Fig. 9a, the translational temperature of atomic hydrogen in the nozzle exit plane is shown. By comparison with Fig. 8b, it is clear that the peak translational temperature is reduced by about 600 K when there is no ohmic heating. Clearly, these DSMC results offer much poorer agreement with the data compared to those obtained with the ohmic heating model. In Fig. 9b, the translational, rotational, and vibrational temperatures predicted in this case are compared with the measurements for rotational temperature. The vibrational temperature is slightly higher in this case due to slower relaxation caused by the reduction in translational temperature. The rotational temperature is lower than that obtained with the ohmic heating model. Once again, the agreement with the data obtained without ohmic heating appears to be worse than that shown in Fig. 8c. The profile of electron temperature in the nozzle exit plane is compared with the measured data in Fig. 9c. In this case, the peak electron temperature predicted by the simulation is only about 2,000 K and is clearly much lower than the values observed experimentally.

Effect of Viscosity

A final simulation is performed in which the momentum cross-sections for interaction between the neutral atoms and molecules are those employed in the earlier DSMC study of a cold flow hydrogen arcjet.¹¹ The ohmic heating model is again employed. In general, the DSMC results are found to be relatively insensitive to viscosity. The most pronounced difference arises in velocity. In Fig. 10, the variation of axial velocity along the nozzle for these cross-sections is compared with the experimental data. With this viscosity model, there are more collisions simulated and hence the gas accelerates to a slightly higher velocity offering better correspondence to the data. It is believed that this improved agreement is fortuitous, although it is recognized that the momentum cross-sections of Ref. 12 may not be accurate throughout the arcjet as they are only evaluated to a temperature of 15,000 K whereas the peak temperature in the arcjet flow is about 30,000 K.

Discussion and Conclusions

The first conclusion to be drawn from the comparisons of DSMC predictions and experimental measurements is that the model for ohmic heating appears to represent the plasma physics very well. The increases in the translational, rotational, and electron temperatures obtained with the ohmic heating model all match very well to the experimental data. Also, in terms of the thermal state of the gas, the DSMC results indicate that a strong degree of thermal nonequilibrium exists in the nozzle exit plane of the thruster. It is therefore a recommendation that continuum methods developed for application to arcjet nozzle flows should include finite rates of relaxation for the vibrational energy of molecular hydrogen, and a separate energy equation for the translational motion of the electrons. These are important loss mechanisms for thruster performance and may explain why continuum methods that omit these processes tend to predict higher values for specific impulse in comparison to experimental data.⁵

It is also clear from the present investigation that the simple approximation that ensures charge neutrality is insufficient. It is hypothesized that this approximation is responsible for the poor prediction by the numerical method of both velocity and electron concentration. Inside the arcjet, the electrons will have very large thermal speeds that would separate them rapidly from the ions. However, electrostatic forces tend to pull the electrons back towards the ions, and at the same time accelerate the ions towards the electrons. This physical phenomena is clearly not captured in sufficient detail by the present approach of moving the electrons with the average ion velocity. This completely omits the particle acceleration. Simulation of this physical behavior would result in the electrons moving through the flow at significantly higher velocities that would in turn decrease the electron number density throughout the nozzle flow. Collision of the accelerated ions and electrons with neutral particles would also result in small increases in the fluid velocity throughout the nozzle flow. In addition, it is anticipated that such an approach would also lead to an increase in the specific impulse computed by the simulation method.

As stated in the earlier discussions, the main difficulty associated with direct inclusion of the electric field effects is the large disparity in length and time scales between plasma and collision processes. In the present investigation, the computational grid is sized according to the collision length scales. For the electron number densities found at the nozzle throat of the arcjet, the cells there would have to be decreased by a factor of 1000 to adequately resolve the plasma behavior. This represents a problem therefore that cannot simply be resolved using supercomputers.

Acknowledgments

This work is funded by the Air Force Office of Scientific Research under grant F49620-94-1-0328 with Dr. Mitat A. Birkan as technical monitor. Contributions to this work by the following are gratefully acknowledged: Bill Butler, Mark Cappelli, Jeff Pobst, Vic Storm, Vish Subramaniam, and Ingrid Wysong.

References

¹ Smith, W. W., Smith, R. D., Davies, S., and Lichtin, D., "Low Power Hydrazine Arcjet System Flight Qualification," Paper 91-148, 22nd International Electric Propulsion Conference, Viareggio, Italy, October

1991.

² Curran, F. M., Bullock, S. R., Haag, T. W., Sarmiento, C. J., and Sankovic, J. M., "Medium Power Hydrogen Arcjet Performance," AIAA Paper 91-2227, June 1991.

³ Liebeskind, J. G., Hanson, R. K., and Cappelli, M. A., "Laser-Induced Fluorescence Diagnostic for Temperature and Velocity Measurements in a Hydrogen Arcjet Plume," *Journal of Applied Optics*, Vol. 32, 1993, pp. 6117-6121.

⁴ Pobst, J. A., Wysong, I. J., and Spores, R. A., "Laser Induced Fluorescence of Ground State Hydrogen Atoms in an Arcjet Plume," AIAA Paper 95-1973, June 1995.

⁵ Butler, G. W., Boyd, I. D., and Cappelli, M. A., "Non-Equilibrium Flow Phenomena in Low Power Hydrogen Arcjets," AIAA Paper 95-2819, July 1995.

⁶ Miller, S. A., "Multifluid Nonequilibrium Simulation of Arcjet Thrusters," Ph. D. thesis, Department of Aeronautics and Astronautics, Massachusetts Institute of Technology, February 1994.

⁷ Rhodes, R. and Keefer, D., "Non-Equilibrium Modeling of Hydrogen Arcjet thrusters," International Electric Propulsion Conference, Paper 93-217, September 1993.

⁸ Aithal, S. M., Subramaniam, V. V., and Babu, V., "Numerical Simulation of Plasma and Reacting Flows," AIAA Paper 96-2024, June, 1996.

⁹ Boyd, I. D. and Stark, J. P. W., "Modelling of a Small Hydrazine Thruster Plume in the Transition Flow Regime," *Journal of Propulsion and Power*, Vol. 6, 1990, pp. 121-126.

¹⁰ Boyd, I. D., Penko, P. F., Meissner, D. L., and DeWitt, K. J., "Experimental and Numerical Investigations of Low-Density Nozzle and Plume Flows of Nitrogen," *AIAA Journal*, Vol. 30, 1992, pp. 2453-2461.

¹¹ Boyd, I. D., Beattie, D. R., and Cappelli, M. A., "Numerical and Experimental Investigations of Low-density Supersonic Jets of Hydrogen," *Journal of Fluid Mechanics*, Vol. 280, 1994, pp. 41-67.

¹² Vanderslice, J. T., Weissman, S., Mason, E. A., and Fallon, R. J., "High-Temperature Transport Properties of Dissociating Hydrogen," *Physics of Fluids*, Vol. 5, 1962, pp. 155-164.

¹³ Bird, G. A., "Monte Carlo Simulation in an Engineering Context," in *Proceedings of 12th Int. Symp. on Rarefied Gas Dynamics*, AIAA, New York, 1981, p. 239.

¹⁴ Crompton, R. W. and Sutton, D. J., "Experimental Investigation of the Diffusion of Slow Electrons in Nitrogen and Hydrogen," *Proceedings of the Royal Society*, Vol. A215, 1952, pp. 467-480.

¹⁵ Yos, J. M., "Transport Properties of Nitrogen, Hydrogen, Oxygen, and Air to 30,000 K," AVCO Research and Advanced Development Technical Memorandum 63-7, 1963.

¹⁶ Borgnakke, C. and Larsen, P. S., "Statistical Collision Model for Monte Carlo Simulation of Polyatomic Gas Mixture," *Journal of Computational Physics*, Vol. 18, 1975, pp. 405-420.

¹⁷ Bergemann, F. and Boyd, I. D., "DSMC Simulation of Inelastic Collisions Using the Borgnakke-Larsen Method Extended to Discrete Distributions of Vibrational Energy," in *Proc. 18th Int. Symp. Rarefied Gas Dynamics*, AIAA, Washington, 1994, Vol. 158, p. 174.

¹⁸ Kiefer, J. H., *Journal of Chemical Physics*, Vol. 57, 1962, p. 1938.

- ¹⁹ NIST Chemical Kinetics Database, Version 5.0, NIST, Gaithersburg, MD.
- ²⁰ McCay, T. D. and Dexter, C. E., "Chemical Kinetic Performance Losses for a Hydrogen Laser Thermal Thruster," *Journal of Spacecraft and Rockets*, Vol. 24, 1987, pp. 372-376.
- ²¹ Boyd, I. D., "Analysis of Vibration-Dissociation-Recombination Processes Behind Strong Shock Waves of Nitrogen," *Physics of Fluids A*, Vol. 4, 1992, pp. 178-184.
- ²² Birdsall, C. K. and Langdon, A. B., *Plasma Physics Via Particle Simulation*, Hilger, Bristol, England, 1991.
- ²³ Boyd, I. D. "Vectorization of a Monte Carlo Method For Nonequilibrium Gas Dynamics," *Journal of Computational Physics*, Vol. 96, 1991, pp. 411-427.
- ²⁴ Wysong, I. J., Pobst, J. A., and Boyd, I. D., "Comparison of Hydrogen Atom Measurements in an Arcjet Plume with DSMC Predictions," AIAA Paper 96-3185, July 1996.
- ²⁵ Boyd, I. D., "Monte Carlo Simulation of Arcjet Plumes," AIAA Paper 96-3297, July 1996.
- ²⁶ Beattie, D.R. and Cappelli, M.A., "Molecular Hydrogen Raman Scattering in a Low Power Arcjet Thruster," AIAA Paper 92-3566, Nashville, Tennessee, July 1992.
- ²⁷ Storm, P. V. and Cappelli, M. A., "Stark Broadening Corrections to Laser-Induced Fluorescence Temperature Measurements in a Hydrogen Arcjet Plume," *Applied Optics*, accepted for publication.
- ²⁸ Storm, P. V. and Cappelli, M. A., "High Spectral Resolution Emission Study of a Low Power Hydrogen Arcjet Plume," AIAA Paper 95-1960, June 1995.
- ²⁹ Storm, P. V. and Cappelli, M. A., "Fluorescence Velocity Measurements in the Interior of a Hydrogen Arcjet Nozzle," *AIAA Journal*, Vol. 34, 1996, pp. 853-855.

Fig. 1. Schematic diagram of the 1 kW hydrogen arcjet.

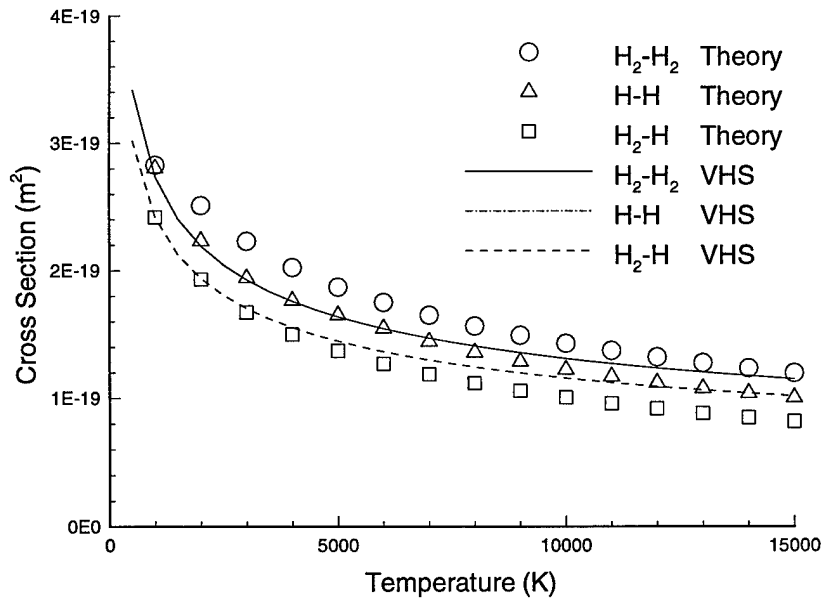


Fig. 2. Average momentum transfer cross-sections as a function of temperature.

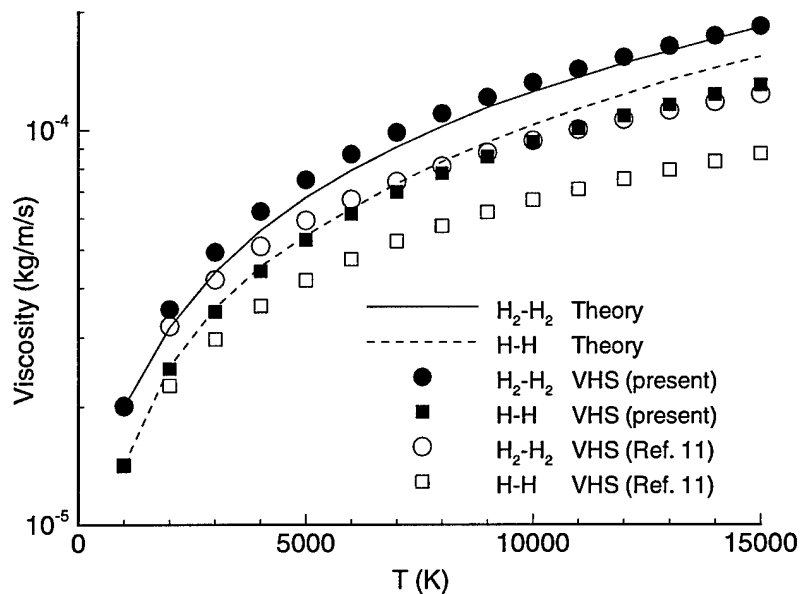


Fig. 3. Viscosity coefficient as a function of temperature.

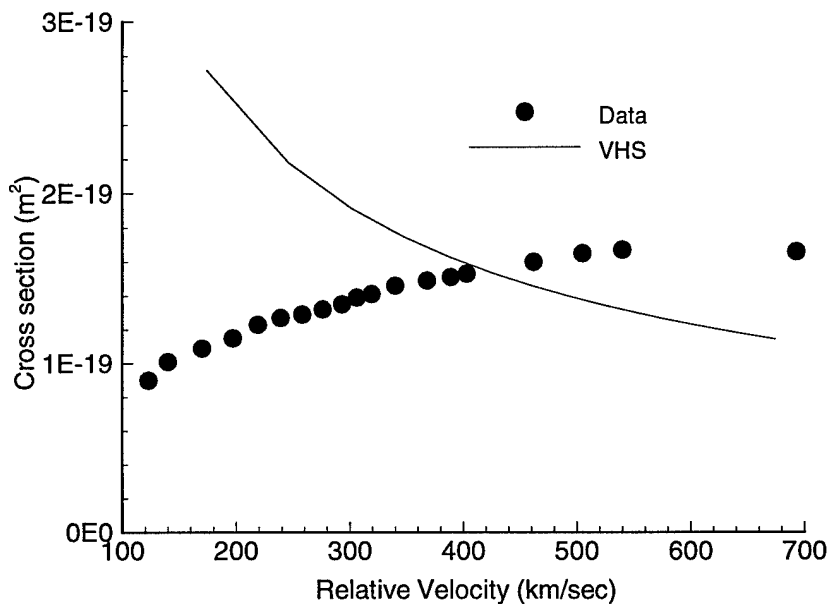


Fig. 4. Momentum transfer cross-sections for H_2-e^- collisions as a function of relative velocity.

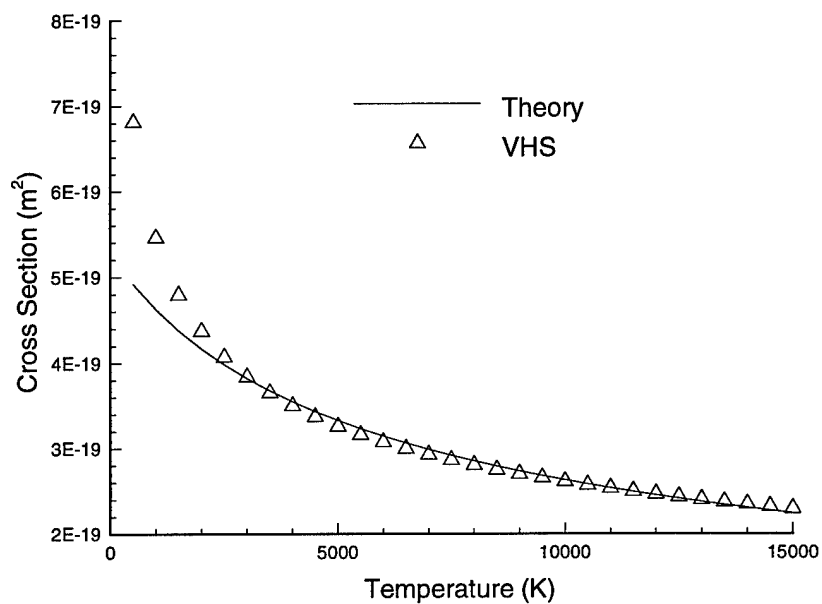


Fig. 5. Momentum transfer cross-sections for H-e⁻ collisions as a function of temperature.

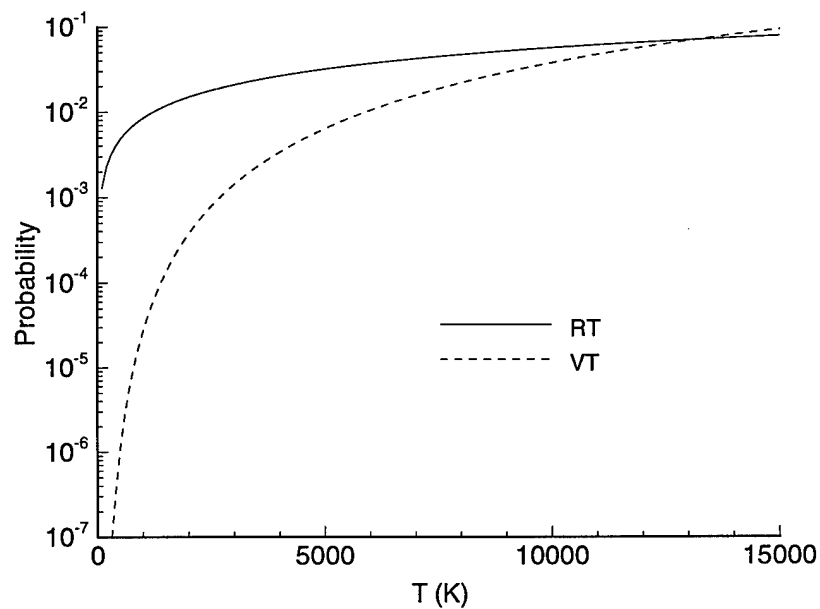


Fig. 6. Average probabilities of RT and VT energy exchange for H₂-H₂ collisions as a function of temperature.

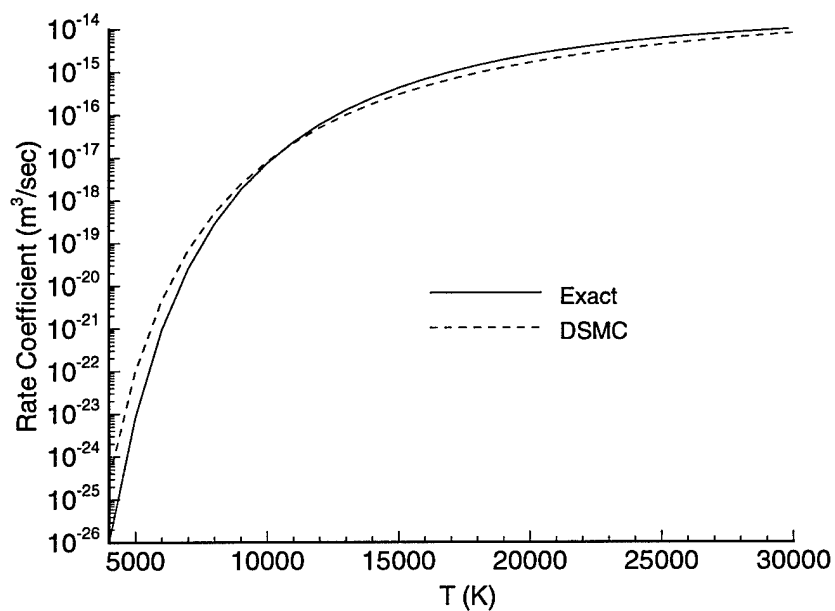


Fig. 7. Rate coefficients for $\text{H} + \text{e}^- \rightarrow \text{H} + \text{H}^+ + \text{e}^-$ as a function of temperature.

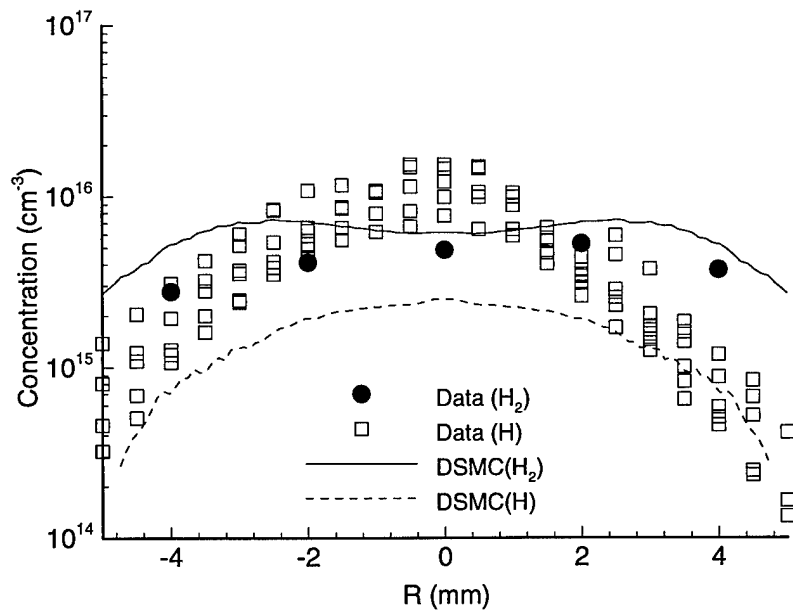


Fig. 8a. Concentrations of neutral species in the nozzle exit plane.

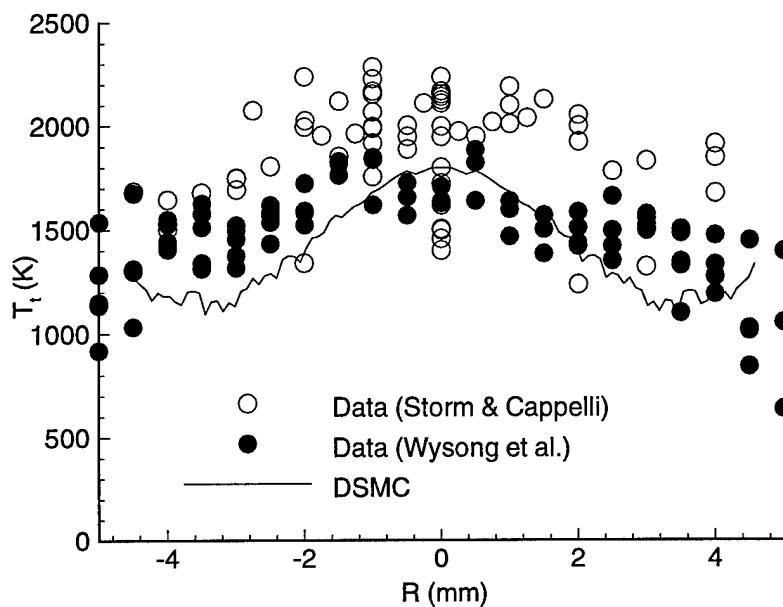


Fig. 8b. Translation temperature of atomic hydrogen in the nozzle exit plane.

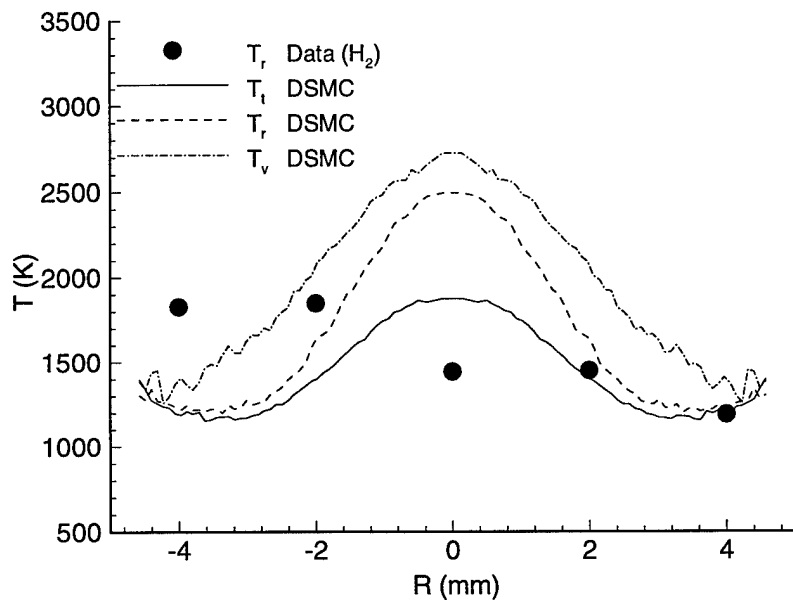


Fig. 8c. Thermal nonequilibrium of molecular hydrogen in the nozzle exit plane.

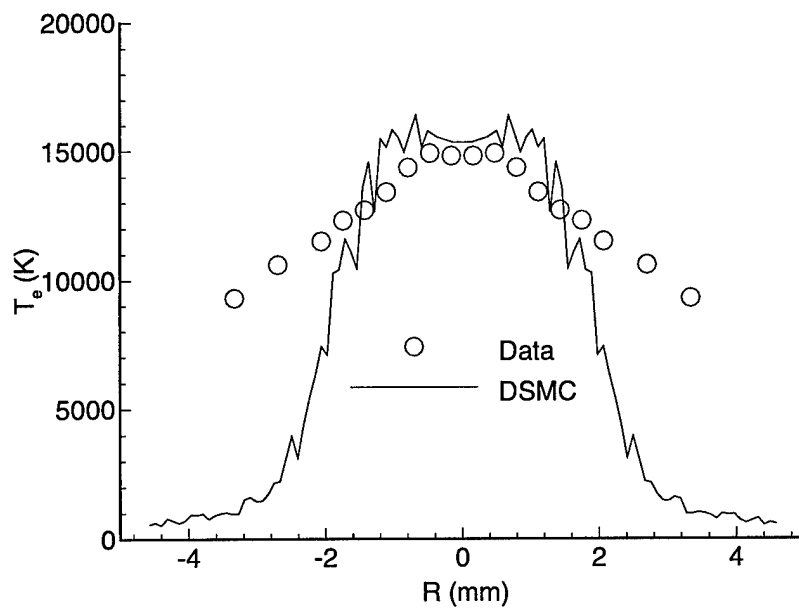


Fig. 8d. Electron temperature in the nozzle exit plane.

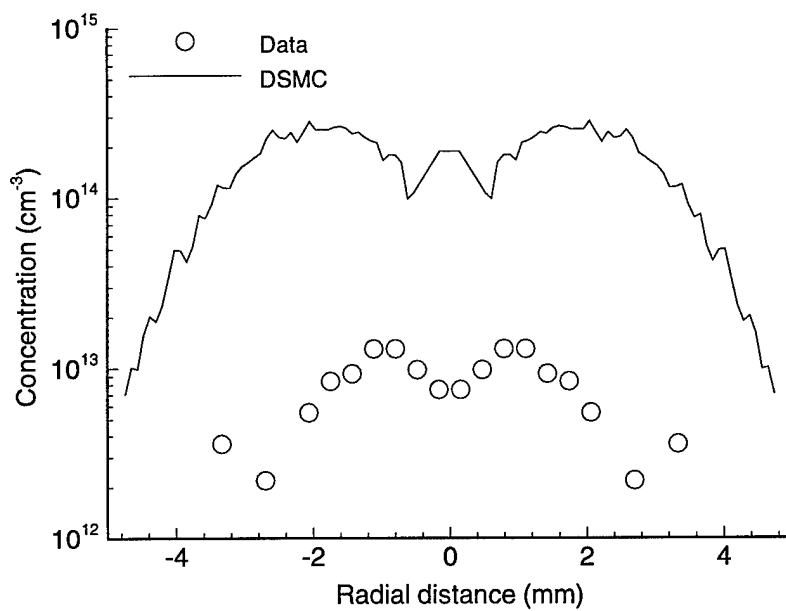


Fig. 8e. Electron concentration in the nozzle exit plane.

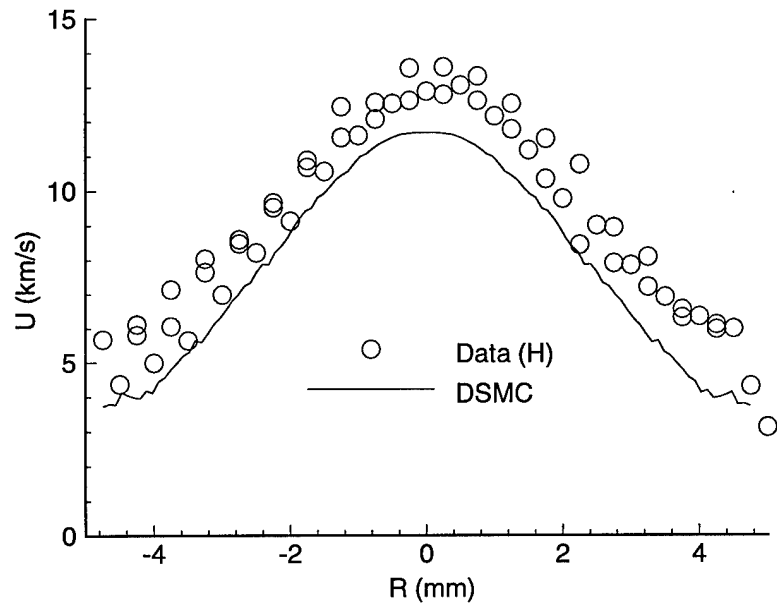


Fig. 8f. Axial velocity component of atomic hydrogen in the nozzle exit plane.

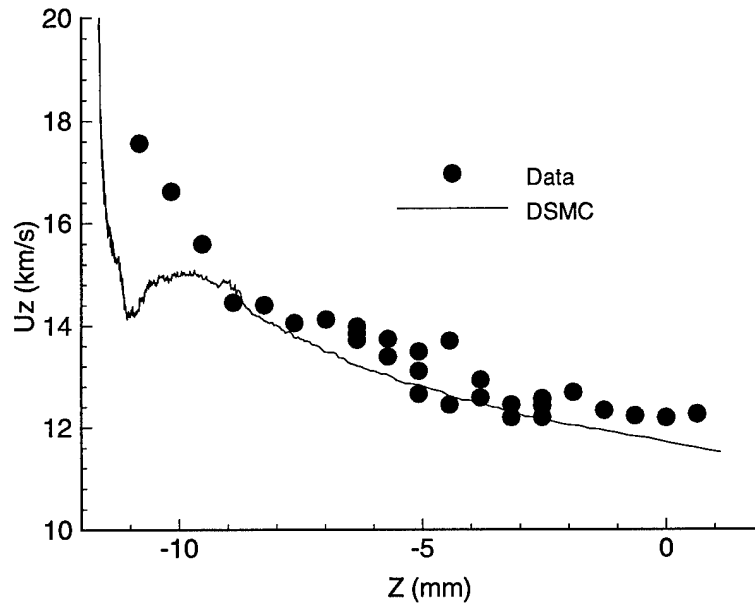


Fig. 8g. Axial velocity component along the nozzle centerline.

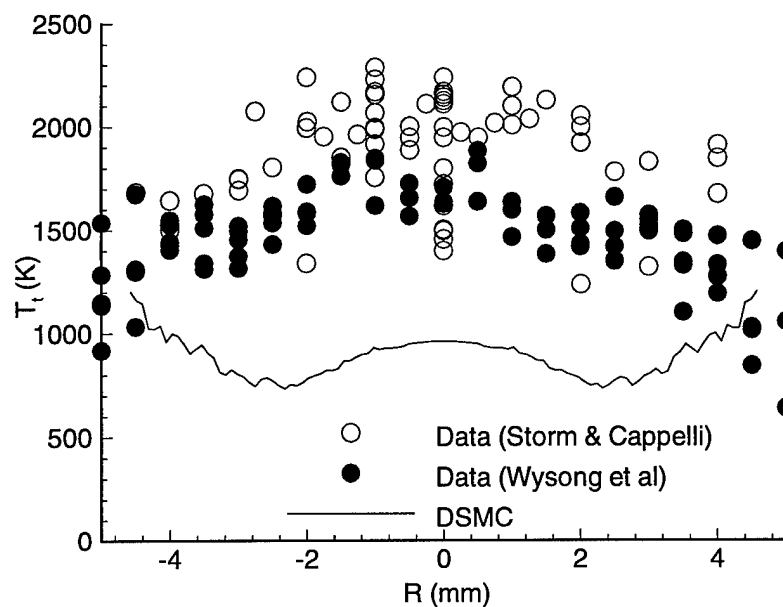


Fig. 9a. Translation temperature of atomic hydrogen in the nozzle exit plane: no ohmic heating.

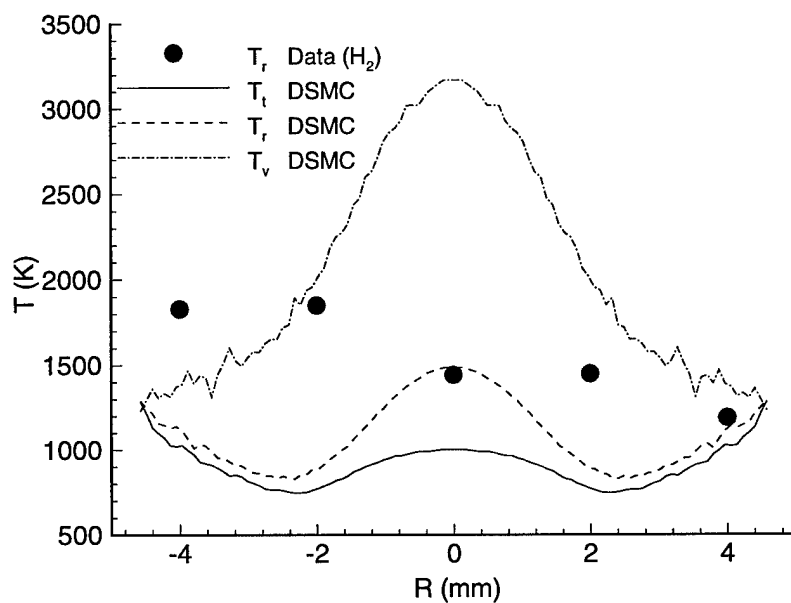


Fig. 9b. Thermal nonequilibrium of molecular hydrogen in the nozzle exit plane: no ohmic heating.

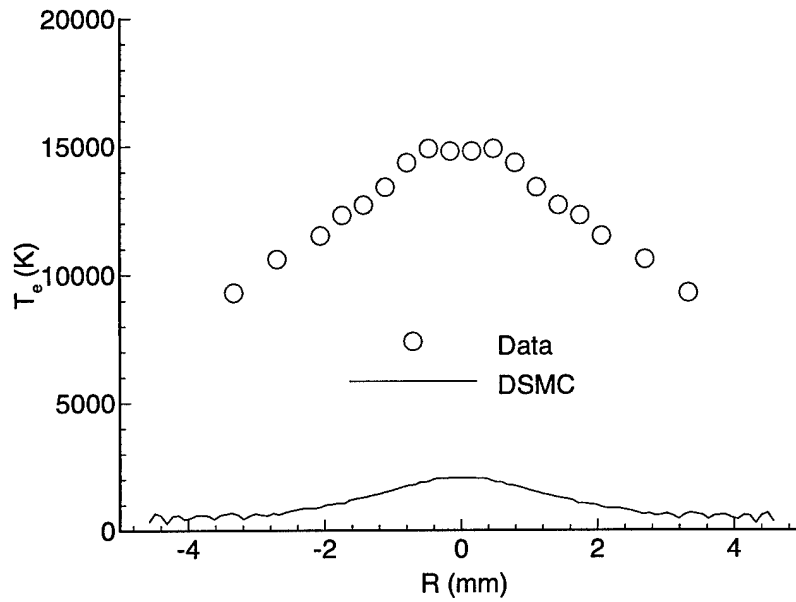


Fig. 9c. Electron temperature in the nozzle exit plane: no ohmic heating.

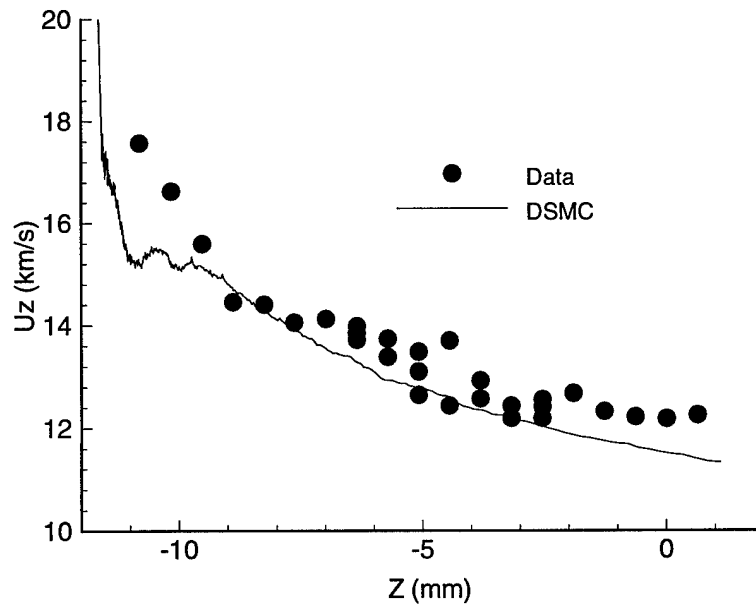


Fig. 10. Axial velocity component along the nozzle centerline: neutral viscosity model of Ref. 11.

II. EXTENSIVE VALIDATION OF THE MONTE CARLO MODEL

Abstract

A particle-based Monte Carlo numerical method is applied to model the nozzle and plume flows of a low-thrust hydrogen arcjet. The method employs the direct simulation Monte Carlo technique to compute the nonequilibrium fluid mechanics and thermochemical relaxation. Simulation of plasma field effects is included at a simple level that ensures charge neutrality. A model is implemented to include ohmic heating in the simulation. Results are presented for two different arcjet flow conditions. Comparisons of Monte Carlo results with experimental measurements of a variety of flow field properties are made in the nozzle interior, in the nozzle exit plane, and in the plume flow field. Comparison of prediction with measurement is also made for thruster performance. In general, good agreement is obtained between simulation and measurement. This indicates that the Monte Carlo model is a viable approach for optimization of arcjet performance, and for estimation of spacecraft interaction effects.

Introduction

Arcjets operated at a power level of about 1 kW are an attractive candidate for use as electric propulsion devices on spacecraft. They offer substantial increases in specific impulse compared with chemical rockets and resistojets. Unfortunately, the performance of arcjets remains poor with propulsion efficiencies in the range of 30 to 50%. There is a need for accurate numerical simulation of the flows generated by these devices both for improving their performance, and for analysis of potential spacecraft interaction effects such as contamination. There are many coupled physical phenomena at work in an arcjet that makes numerical simulation difficult. Nonequilibrium kinetic processes include rotational and vibrational relaxation, and several chemical mechanisms including dissociation, recombination, and ionization. In addition plasma effects are important.

A hydrazine arcjet has been developed and flown in space.¹ In terms of basic research, however, hydrogen arcjets have received considerable attention. Several experimental studies have been conducted on an arc-jet designed and fabricated at NASA Lewis Research Center. A schematic diagram of this thruster is shown in Fig. 1. The NASA Lewis hydrogen arcjet has been used in experimental investigations to determine its performance² and flow fields.³⁻⁴ Of considerable importance is the fact that several different diagnostic techniques have been applied to these flows yielding measurements that include translational and rotational temperature, velocity, and number densities of atomic and molecular hydrogen. These data offer excellent opportunities for detailed calibration of modeling efforts. Arcjet models based on continuum formulations have been developed by several groups.⁵⁻⁸ There are two main problems with the continuum approach. First, there is a significant degree of thermal and chemical nonequilibrium in these flows that may not be simulated accurately using a continuum formulation. Second, it is very difficult to extend the continuum simulations out to the plume produced by the arcjet. This means that these methods cannot be used to predict spacecraft interference effects.

This paper describes the application of the direct simulation Monte Carlo method (DSMC) for computation of the flow fields of a hydrogen arcjet. In satellite propulsion, the DSMC technique has been applied and successfully verified to the plume of a hydrazine rocket⁹, and to the nozzle and plume flows of both a nitrogen resisto-jet¹⁰ and a cold flow of hydrogen through an arcjet.¹¹ In this paper, brief description is provided of the kinetic and plasma models developed for this application. More details may be found in Ref. 12. Extensive comparison of the Monte Carlo calculations with available experimental data is made in the nozzle interior, in the nozzle exit plane, and in the plume expansion flow fields. Comparison is also made with measurement for thruster performance.

Numerical Method

The direct simulation Monte Carlo method (DSMC) uses the motions and collisions of particles to perform a direct simulation of nonequilibrium gas dynamics. Each particle has coordinates in physical space, three velocity components, and internal energies. A computational grid is employed to group together particles that are likely to collide. Collision selection is based on a probability model developed from basic concepts in kinetic theory. The method is widely used for rarefied nonequilibrium conditions and finds application in hypersonics, materials processing, and micro-machine flows.

The extension of the technique for application to arcjet flows is described in detail by Boyd.¹² This required development of a number of new physical models. Arcjets are characterized by high temperatures (as high as 30,000 K) that give rise to strongly ionized flows (as much as 30% ionized). In terms of intermolecular collisions, mechanisms must be included in the numerical model to account for: (1) momentum transfer; (2) rotational excitation; (3) vibrational excitation; (4) dissociation/recombination; and (5) ionization/recombination. The relatively large degree of ionization requires modeling of plasma effects at some level.

For a hydrogen arcjet, the four main species present are H_2 , H , H^+ , and e^- . In general, the most important collision types that determine the arcjet flow field are H_2-H_2 , H_2-H , $H-H$, H_2-e^- , and $H-e^-$. In the present work, the momentum transfer cross-sections for the first three collision types are obtained from the work of Vanderslice et al.¹³ in which collision integrals were tabulated for the temperature range of 1,000 to 15,000 K. The cross-sections for the H_2-e^- collision is determined using the experimental data of Crompton and Sutton.¹⁴ The cross-section for the $H-e^-$ collision is determined using the simple analytical expression given by Yos.¹⁵ The level of agreement between the models used in the DSMC code and the original sources is very good with the exception of the H_2-e^- collision. Other cross-sections are much less important and are assigned values such that the results of hydrogen atoms are used for hydrogen ions. For example, the cross-sections for H_2-H collisions are also used for H_2-H^+ collisions. While this results in some lack of accuracy, it is expected that the effect will be small as these collisions are relatively infrequent.

Molecular hydrogen is an interesting diatomic molecule in that it has relatively large values for the characteristic temperatures of rotation and vibration. This results in long relaxation times for these modes.

Previously, a rate model for determining the probability of translational-rotational energy transfer for hydrogen at low temperatures was developed and verified.¹¹ This same model is employed again here although it is recognized that it may be inaccurate at the very high temperatures encountered in the arcjet. The probability of vibrational energy exchange employs the familiar Landau-Teller relaxation time with parameters obtained experimentally by Kiefer and Lutz.¹⁶ Once again it is recognized that this approach may be inaccurate at the very high temperatures found in the arcjet. There are only two chemical reactions implemented in the present study. They are dissociation of molecular hydrogen and ionization of atomic hydrogen. The rate coefficients are obtained from Refs. 17 and 18.

A very simple scheme is employed to simulate electric field effects. The electrons are constrained to move through the flow field with the average ion velocity in each cell. This ensures charge neutrality, but obviously omits the electric field effects. A second important plasma effect that is included in the DSMC simulation is ohmic heating. This is an important source of energy that results from the current represented by the flux of charged species through the thruster. Using standard plasma physics theory, a source of energy is computed in each cell of the simulation due to ohmic heating. This energy is added to the charged particles in each cell in each iteration of the calculation. The scheme is described in detail in Ref. 12.

The collision and plasma models are implemented in an existing DSMC code that is designed for efficient performance on vector supercomputers.¹⁹ The DSMC computations are begun at a location downstream of the nozzle throat. The initial profiles of flow properties are obtained from continuum simulations provided by the code of Butler.⁵ The interaction of the gas with the wall of the nozzle is assumed to be diffuse with full energy accommodation to the wall temperature profile obtained from the continuum simulation. Charged species are neutralized upon contact with the wall. The computations extend through the nozzle exit plane to a distance of 30 mm from the thruster along the axis. Expansion is assumed to occur into a perfect vacuum.

The grids employed typically consist of 500 by 55 cells. Due to the wide dynamic range in density for these flows, the cells are adapted to the local mean free path, and the time step in each cell is scaled by the local mean time between collisions. Despite the time step variation, the transient phase of the simulation remains long. Typically, it requires at least 15,000 iterations before steady state is reached. Macroscopic results are then obtained by sampling properties over a further 10,000 time steps. At steady state, there are at least 300,000 particles present in the simulation.

Results

Results are presented for a mass flow rate of 13.3 mg/sec and power levels of 1.34 and 0.80 kW. These correspond very closely to conditions considered in a number of experimental investigations. Comparison of DSMC predictions with experimental data for various flow field properties is made at the following locations: (1) in the interior of the nozzle; (2) in the nozzle exit plane; and (3) in the plume flow field. In addition, comparison is made between measurement and prediction for specific impulse.

Nozzle Interior

In Fig. 2a, the variation of axial velocity component along the nozzle centerline is shown at a power of 1.34 kW. The axis labeling is such that an axial coordinate of zero is located at the nozzle exit plane. The experimental data is due to Storm and Cappelli.²⁰ Note that these data were measured at a slightly higher arcjet power of 1.48 kW. The DSMC simulation provides quite good agreement with the data although there is a tendency to predict slightly lower values. This may partly be attributed to the lower power considered in the simulation. Far upstream, the data indicates velocities that are significantly higher than the computed values; however, this is the region of greatest experimental uncertainty. The minimum turning point shown in the DSMC calculations is a result of the diffusion of cold hydrogen molecules from the boundary layer into the hot core region where the plasma deposition of energy is greatest.

Radial profiles of axial velocity component at three different axial locations inside the nozzle are shown in Fig. 2b. In general, the shapes of the measured and predicted profiles are in good agreement and are found to improve with increased downstream distance. In particular, the profile computed at a distance of just -2.54 mm from the nozzle exit plane shows the best agreement with the data.

Nozzle Exit Plane

In Fig. 3a, the concentrations of molecular and atomic hydrogen across the nozzle exit plane are shown. Experimental measurement of H_2 was performed by Beattie and Cappelli²¹ using Raman scattering. The measurements for H are those reported by Wysong et al.²² obtained using a two-photon laser induced fluorescence technique. In general, the agreement between computation and measurement is better for H_2 than for H. In particular, the simulations predict an atomic concentration on the axis that is a factor of 3 to 4 smaller than the experimental data. A further simulation performed with the dissociation rate for H_2 -H collisions increased by a factor of 10 led to an increase in H-atom concentration at the nozzle exit of just 10%. The discrepancy between measurement and calculation for the hydrogen atom concentrations is therefore attributed either to too little dissociation in the continuum solution used to start the DSMC calculation, or to experimental error.

In Fig. 3b, the translational temperature profile of atomic hydrogen across the nozzle exit plane is shown. Two sets of experimental data reported by Wysong et al.²² and by Storm and Cappelli²³ are shown. In general, the DSMC results show a small underprediction of the temperature, although the agreement is quite good. The degree of thermal nonequilibrium of the flow in the nozzle exit is illustrated in Fig. 3c. Here, the translational, rotational, and vibrational temperatures of molecular hydrogen predicted by the DSMC technique are compared with the rotational temperature measurements of Beattie and Cappelli.²¹ The predicted rotational temperatures offer satisfactory agreement with the measured data. The peak vibrational temperature is about 1,000 K higher than the peak translational temperature.

A further indication of the degree of thermal nonequilibrium in this flow is illustrated in Fig. 3d in which the electron temperature at the nozzle exit plane is shown. The experimental data is due to Storm and Cappelli.²⁴ There are two DSMC results shown in which the effect of including ohmic dissipation

(Ω) is considered. With ohmic dissipation, there is quite good agreement obtained with the experimental data. By comparison, omission of Ω leads to significant underprediction of the electron temperature. Note that with ohmic heating, the peak electron temperature is an order of magnitude higher than the peak translational temperature, again illustrating the strong degree of thermal nonequilibrium in these flows. In Fig. 3e, the electron concentration across the nozzle exit plane is shown. The experimental data was also reported in Ref. 24. The agreement between simulation and measurement is very poor with the DSMC technique predicting concentrations that are an order of magnitude higher than the data. This behavior is attributed to the very simple model employed in the DSMC computation for simulating the electric field effects. Remember, the electrons are constrained to move with the average ion velocity, and this is obviously much slower than would occur in the actual flow.

Finally, the axial component of velocity in the nozzle exit plane is shown in Fig. 3f. The experimental data is that of Wysong et al.²² While offering relatively good agreement, the DSMC results are consistently lower than the measured data across most of the exit plane. The shape of the velocity profile is captured very well by the simulation.

In Figs. 4a-4d, comparisons of simulation and data for a power level of 0.80 kW are shown for neutral species concentrations, translational temperature of hydrogen atoms, internal temperatures of hydrogen molecules, and axial velocity component of hydrogen atoms. Overall, the same observations hold at this power level as for the 1.34 kW case. The agreement between simulation and measurement is generally very good except for the hydrogen atom concentrations in which the DSMC technique predicts densities that are a factor of about 3 lower than the experimental data.

Plume Flow Field

Of the many experimental investigations of hydrogen arcjet flows, Ref. 22 is unique in that data taken in the plume are reported that are unaffected by chamber effects are reported. These data are compared in this section with the corresponding DSMC results out to a distance of 30 mm from the nozzle exit plane. Variation of translational temperature and axial velocity component for atomic hydrogen along the axis of the plume are shown in Figs. 5a and 5b for a power level of 1.34 kW. In these plots, the axis labeling is such that the nozzle exit plane is again located at zero. It should be noted that these are the first comparisons between simulation and measurement conducted in the plume of an arcjet thruster. As shown in Fig. 5a, the temperature profile predicted by the DSMC technique is in excellent agreement with the experimental data. For velocity, the DSMC results lie consistently 1-2 km/s below the data; however, it is significant that the lack of change in velocity is predicted by the simulation.

Axial plume profiles of translational temperature and axial velocity component at a power level of 0.80 kW are shown in Figs. 6a and 6b. In this case, the DSMC temperature predictions are distinctly lower than the measured data. The velocity predictions are again lower than the experimental results by 1-2 km/s.

In the experimental investigation of Wysong et al.²², radial profiles of plume properties were also measured at an axial distance of 10 mm from the nozzle exit plane. In Figs. 7a and 7b profiles of translational

temperature and axial velocity component of atomic hydrogen are shown for a power of 1.34 kW. Within the large scatter exhibited by the measurements, the peaked profile predicted by the DSMC technique offers reasonable agreement. The velocity profiles are in excellent agreement.

In Figs. 8a and 8b, the temperature and velocity profiles for a power of 0.80 kW are shown. The DSMC method predicts significantly lower temperatures and slightly lower velocities.

Axial and radial profiles of hydrogen atom concentration were also measured in Ref. 22. The comparisons of those data with the DSMC predictions are consistent with the behavior at the nozzle exit plane. Thus, in a fairly consistent way, the DSMC method predicts densities for hydrogen atoms throughout the plume that are a factor of 3 to 4 lower than the measured data.

Thruster Performance

Validation of DSMC predictions for flow field properties is important for assessment of spacecraft interaction effects such as contamination. However, an equally important role for numerical simulations lies in the optimization of arcjet design. For computational methods to be taken seriously in this respect, it is essential that they are able to accurately predict overall thruster performance. A series of measurements of the thrust obtained from the hydrogen arcjet under different operating conditions and geometries was conducted several years ago at NASA Lewis Research Center.² The data employed here for comparison with the DSMC results is for the arcjet configuration that most closely resembled that employed in the flow field measurements and simulations. In Fig. 9, variation of specific impulse with specific energy (power/flow rate) is shown. Experimental data is provided at two different flow rates that bound the condition considered in the simulations. Two sets of DSMC data are shown that indicate the effect of including ohmic dissipation in the simulation. As expected, with finite Ω , the specific impulse is increased, and the amount of the increase appears to grow with specific energy. Due to the scatter in the measurements and the fact that the flow rates are different from the simulation, it is difficult to make a definitive comparison. However, it does appear that the DSMC predictions that include ohmic heating agree with the measured data to within 5%. Further computations need to be undertaken to cover a wider range of operating conditions.

Concluding Remarks

A Monte Carlo method has been developed and applied to simulate flow in the nozzle and plume of a hydrogen arcjet. The model includes detailed simulation of nonequilibrium collision and plasma phenomena. These models are implemented in a numerically efficient computer code. In this study, extensive comparison between code predictions and a variety of experimental measurements were presented. The comparisons were made for two different arcjet power levels, and for several different aspects of the arcjet flow fields. In particular, predicted results were compared with measured data in the nozzle interior, at the nozzle exit plane, and in the plume expansion. Monte Carlo prediction of specific impulse was also compared with experimental measurement.

In terms of the arcjet flow fields, there was generally good agreement between prediction and measure-

ment for both translational temperature and velocity. There was an overall tendency in the simulations to predict slightly lower values of temperature and velocity in comparison with the experimental results. The greatest discrepancy occurred for the concentration of atomic hydrogen for which the Monte Carlo approach predicted values that were a factor of 3 to 4 lower than those measured. This behavior was found to be consistent at the nozzle exit and throughout the plume flow field. A significant increase in the hydrogen dissociation rate employed in the simulation did not increase the hydrogen atom concentration significantly. Therefore, it is postulated that the discrepancy lies either in the starting conditions employed in the Monte Carlo calculations, or in the calibration of the diagnostic technique.

At the nozzle exit plane, the nozzle expansion process has created a flow that is in a state of strong thermal nonequilibrium. The Monte Carlo simulation predicts different values of temperature for the translational, rotational, and vibrational energy modes, and for the electrons. In terms of the electrons, it is demonstrated that a model is required to simulate ohmic heating in order to accurately predict the electron temperature profiles measured experimentally. It was also found that a simple model employed to simulate electric field effects results in prediction of electron concentrations that were too high by about an order of magnitude.

For thruster performance, the Monte Carlo simulation is able to reproduce experimental measurements within about 5% when ohmic heating is included in the computation.

In summary, the generally successful comparisons between prediction and measurement of flow field properties indicates that the Monte Carlo method is capable of computing hydrogen arcjet flows with engineering accuracy. This has the significance of demonstrating that the numerical method may be used for prediction of spacecraft interaction effects when arcjets are employed on real satellite configurations. The good agreement obtained between computation and measurement for specific impulse demonstrates that the Monte Carlo method may be employed for optimization of the performance of hydrogen arcjets.

Additional research on the treatment in the Monte Carlo approach of electric field effects should lead to even better correspondence between prediction and measurement for both flow field properties and thruster performance. For application of the Monte Carlo method to the hydrazine arcjets that are flown in space, work is also needed to develop appropriate models for this more complicated thermochemical nonequilibrium system.

Acknowledgments

This work is funded by the Air Force Office of Scientific Research under grant F49620-94-1-0328 with Dr. Mitat A. Birkan as technical monitor. Contributions to this work by the following are gratefully acknowledged: Bill Butler, Mark Cappelli, Jeff Pobst, Vic Storm, Vish Subramaniam, and Ingrid Wysong.

References

- ¹ Smith, W. W., Smith, R. D., Davies, S., and Lichtin, D., "Low Power Hydrazine Arcjet System Flight Qualification," Paper 91-148, 22nd International Electric Propulsion Conference, Viareggio, Italy, October 1991.
- ² Curran, F. M., Bullock, S. R., Haag, T. W., Sarmiento, C. J., and Sankovic, J. M., "Medium Power Hydrogen Arcjet Performance," AIAA Paper 91-2227, June 1991.
- ³ Liebeskind, J. G., Hanson, R. K., and Cappelli, M. A., "Laser-Induced Fluorescence Diagnostic for Temperature and Velocity Measurements in a Hydrogen Arcjet Plume," *Journal of Applied Optics*, Vol. 32, 1993, pp. 6117-6121.
- ⁴ Pobst, J. A., Wysong, I. J., and Spores, R. A., "Laser Induced Fluorescence of Ground State Hydrogen Atoms in an Arcjet Plume," AIAA Paper 95-1973, June 1995.
- ⁵ Butler, G. W., Boyd, I. D., and Cappelli, M. A., "Non-Equilibrium Flow Phenomena in Low Power Hydrogen Arcjets," AIAA Paper 95-2819, July 1995.
- ⁶ Miller, S. A., "Multifluid Nonequilibrium Simulation of Arcjet Thrusters," Ph. D. thesis, Department of Aeronautics and Astronautics, Massachusetts Institute of Technology, February 1994.
- ⁷ Rhodes, R. and Keefer, D., "Non-Equilibrium Modeling of Hydrogen Arcjet thrusters," International Electric Propulsion Conference, Paper 93-217, September 1993.
- ⁸ Aithal, S. M., Subramaniam, V. V., and Babu, V., "Numerical Simulation of Plasma and Reacting Flows," AIAA Paper 96-2024, June, 1996.
- ⁹ Boyd, I. D. and Stark, J. P. W., "Modelling of a Small Hydrazine Thruster Plume in the Transition Flow Regime," *Journal of Propulsion and Power*, Vol. 6, 1990, pp. 121-126.
- ¹⁰ Boyd, I. D., Penko, P. F., Meissner, D. L., and DeWitt, K. J., "Experimental and Numerical Investigations of Low-Density Nozzle and Plume Flows of Nitrogen," *AIAA Journal*, Vol. 30, 1992, pp. 2453-2461.
- ¹¹ Boyd, I. D., Beattie, D. R., and Cappelli, M. A., "Numerical and Experimental Investigations of Low-density Supersonic Jets of Hydrogen," *Journal of Fluid Mechanics*, Vol. 280, 1994, pp. 41-67.
- ¹² Boyd, I. D., "Monte Carlo Simulation of Nonequilibrium Flow In Low Power Hydrogen Arcjets," AIAA Paper 96-2022, June 1996.
- ¹³ Vanderslice, J. T., Weissman, S., Mason, E. A., and Fallon, R. J., "High-Temperature Transport Properties of Dissociating Hydrogen," *Physics of Fluids*, Vol. 5, 1962, pp. 155-164.
- ¹⁴ Crompton, R. W. and Sutton, D. J., "Experimental Investigation of the Diffusion of Slow Electrons in Nitrogen and Hydrogen," *Proceedings of the Royal Society*, Vol. A215, 1952, pp. 467-480.

- ¹⁵ Yos, J. M., "Transport Properties of Nitrogen, Hydrogen, Oxygen, and Air to 30,000 K," AVCO Research and Advanced Development Technical Memorandum 63-7, 1963.
- ¹⁶ Kiefer, J. H. and Lutz, J. H., "Vibrational Relaxation of Hydrogen," *Journal of Chemical Physics*, Vol. 44, 1966, pp. 668-672.
- ¹⁷ *NIST Chemical Kinetics Database, Version 5.0*, NIST, Gaithersburg, MD.
- ¹⁸ McCay, T. D. and Dexter, C. E., "Chemical Kinetic Performance Losses for a Hydrogen Laser Thermal Thruster," *Journal of Spacecraft and Rockets*, Vol. 24, 1987, pp. 372-376.
- ¹⁹ Boyd, I. D. "Vectorization of a Monte Carlo Method For Nonequilibrium Gas Dynamics," *Journal of Computational Physics*, Vol. 96, 1991, pp. 411-427.
- ²⁰ Storm, P. V. and Cappelli, M. A., "Fluorescence Velocity Measurements in the Interior of a Hydrogen Arcjet Nozzle," *AIAA Journal*, Vol. 34, 1996, pp. 853-855.
- ²¹ Beattie, D.R. and Cappelli, M.A., "Molecular Hydrogen Raman Scattering in a Low Power Arcjet Thruster," AIAA Paper 92-3566, Nashville, Tennessee, July 1992.
- ²² Wysong, I. J., Pobst, J. A., and Boyd, I. D., "Comparison of Hydrogen Atom Measurements in an Arcjet Plume with DSMC Predictions," AIAA Paper 96-3185, July 1996.
- ²³ Storm, P. V. and Cappelli, M. A., "Stark Broadening Corrections to Laser-Induced Fluorescence Temperature Measurements in a Hydrogen Arcjet Plume," *Applied Optics*, accepted for publication.
- ²⁴ Storm, P. V. and Cappelli, M. A., "High Spectral Resolution Emission Study of a Low Power Hydrogen Arcjet Plume," AIAA Paper 95-1960, June 1995.

Fig. 1. Schematic diagram of the 1 kW hydrogen arcjet.

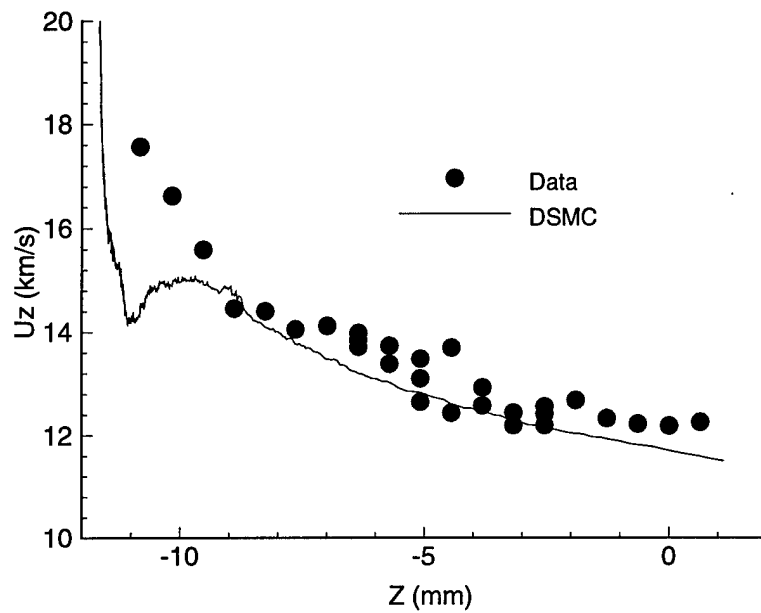


Fig. 2a. Axial velocity component along the nozzle centerline for $P=1.34$ kW.

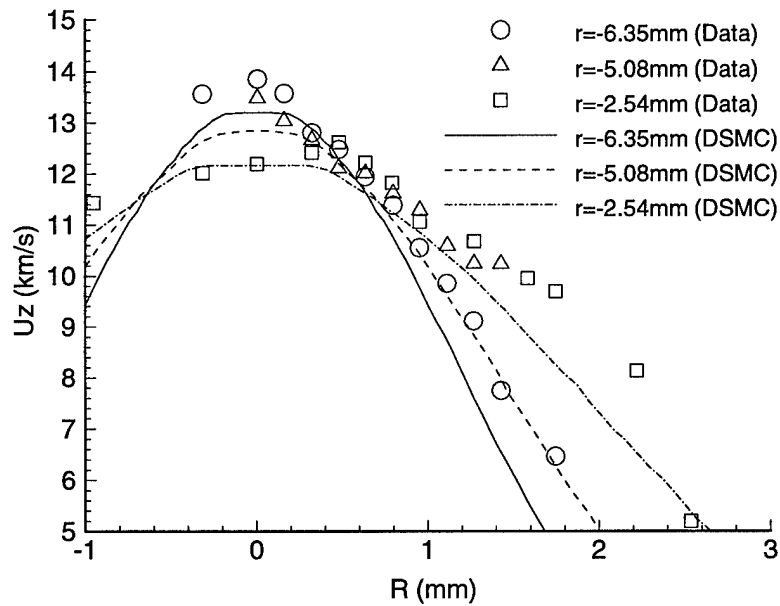


Fig. 2b. Radial profiles of axial velocity component at different axial locations in the nozzle for $P=1.34$ kW.

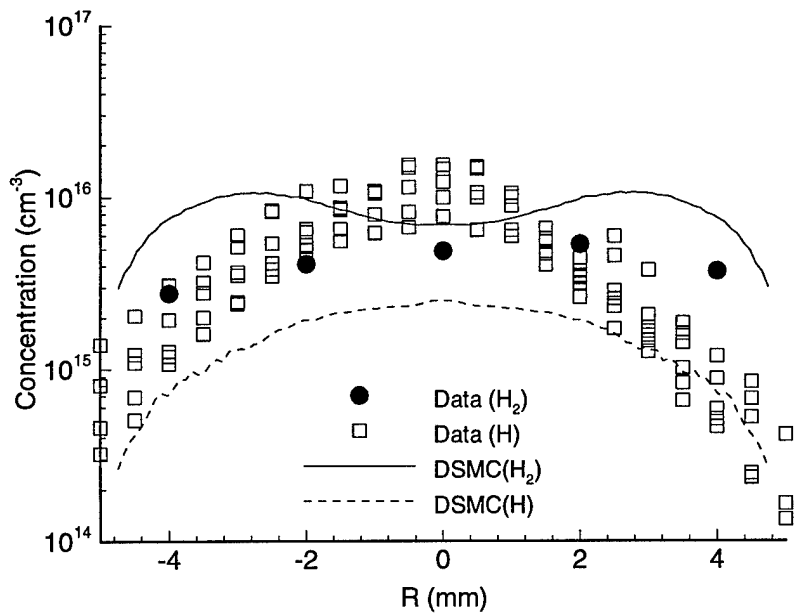


Fig. 3a. Concentrations of neutral species in the nozzle exit plane for $P=1.34$ kW.

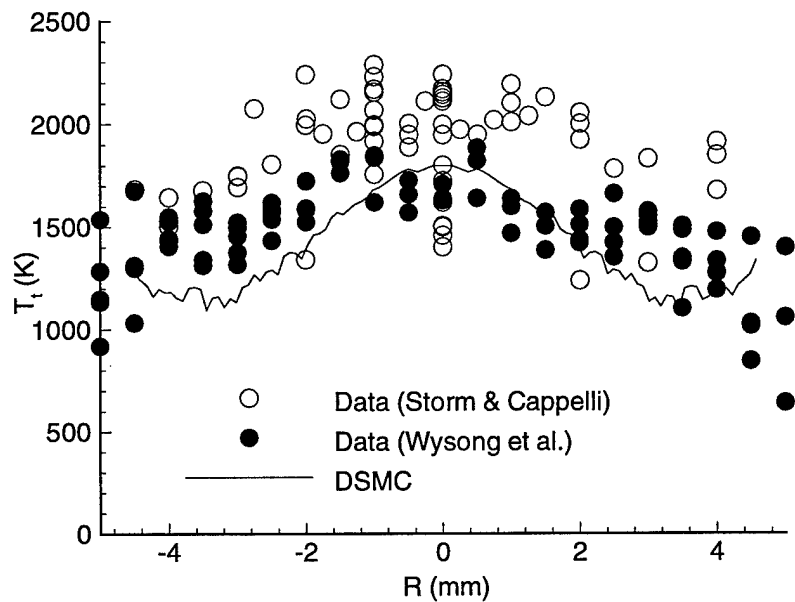


Fig. 3b. Translational temperature of atomic hydrogen in the nozzle exit plane for $P=1.34$ kW.

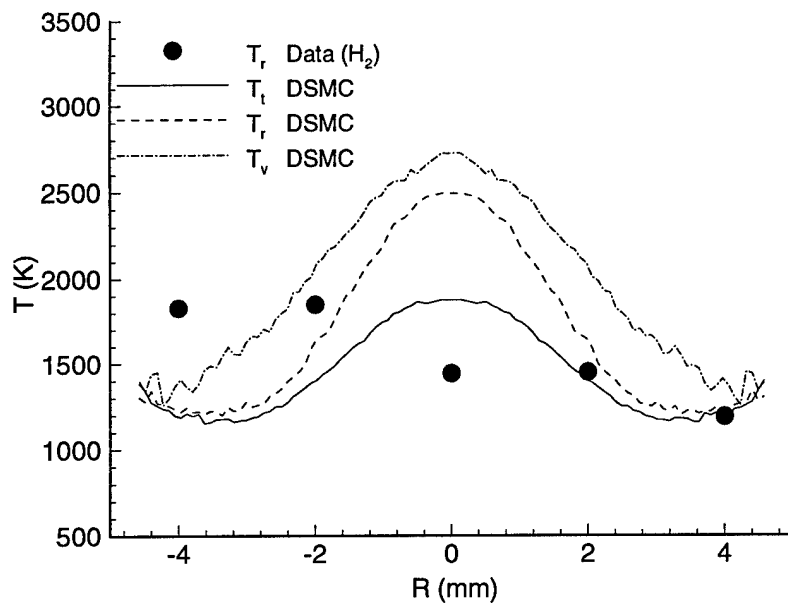


Fig. 3c. Thermal nonequilibrium of molecular hydrogen in the nozzle exit plane for $P=1.34$ kW.

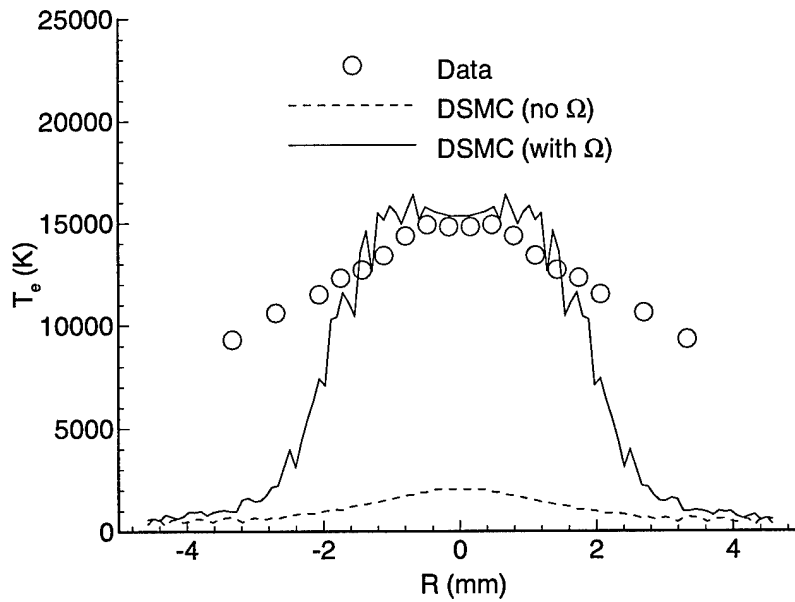


Fig. 3d. Electron temperature in the nozzle exit plane for $P=1.34$ kW.

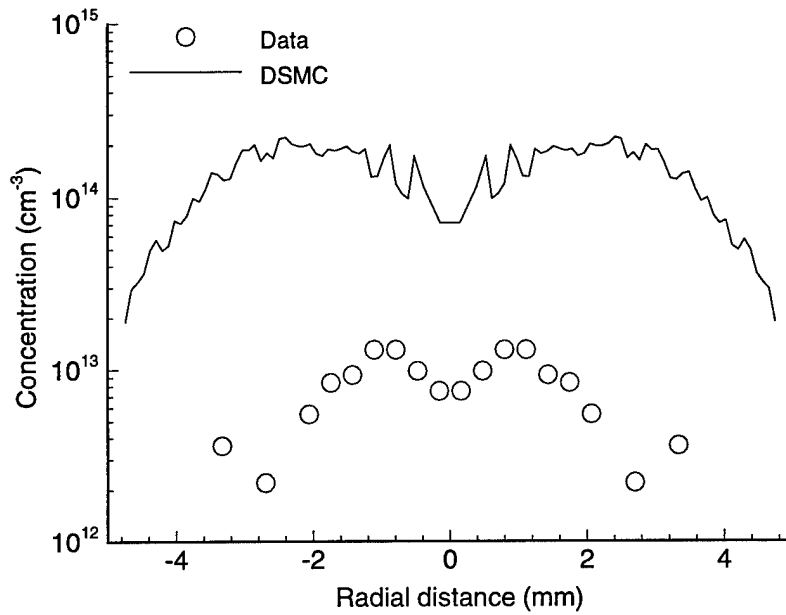


Fig. 3e. Electron concentration in the nozzle exit plane for P=1.34 kW.

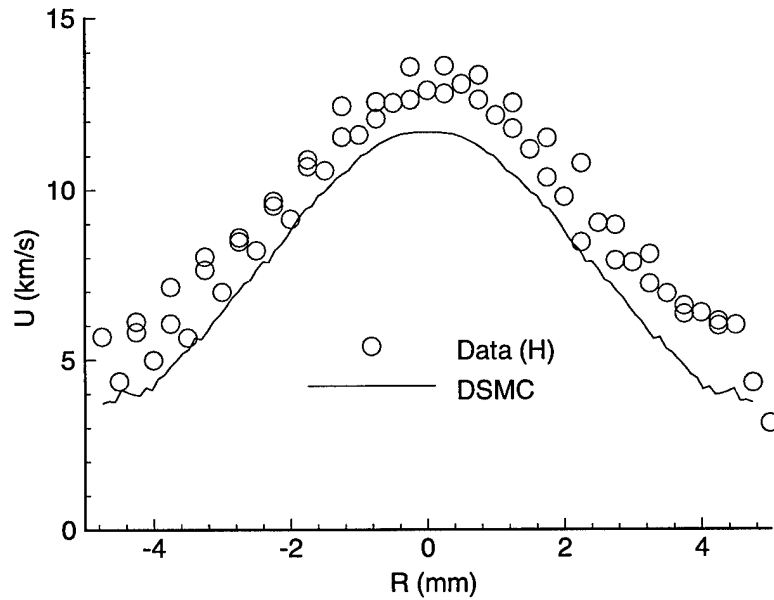


Fig. 3f. Axial velocity component of atomic hydrogen in the nozzle exit plane for P=1.34 kW.

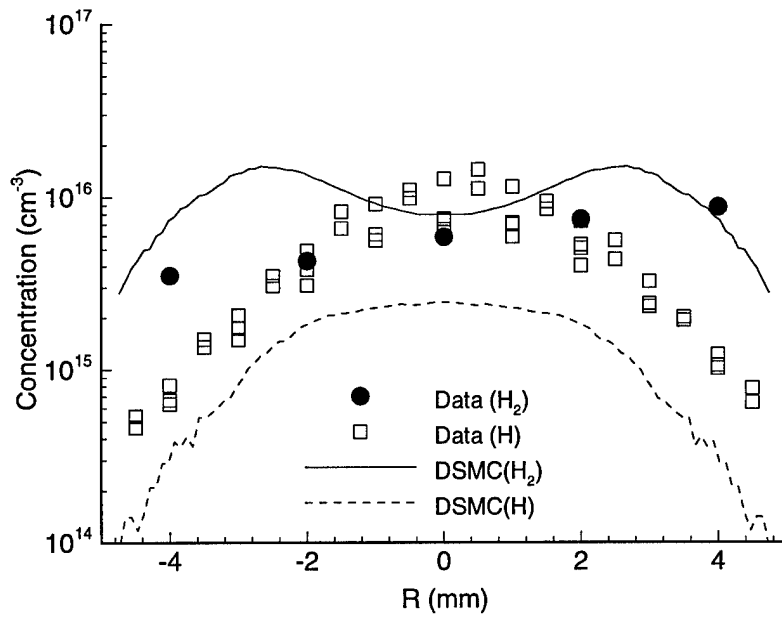


Fig. 4a. Concentrations of neutral species in the nozzle exit plane for $P=0.80$ kW.

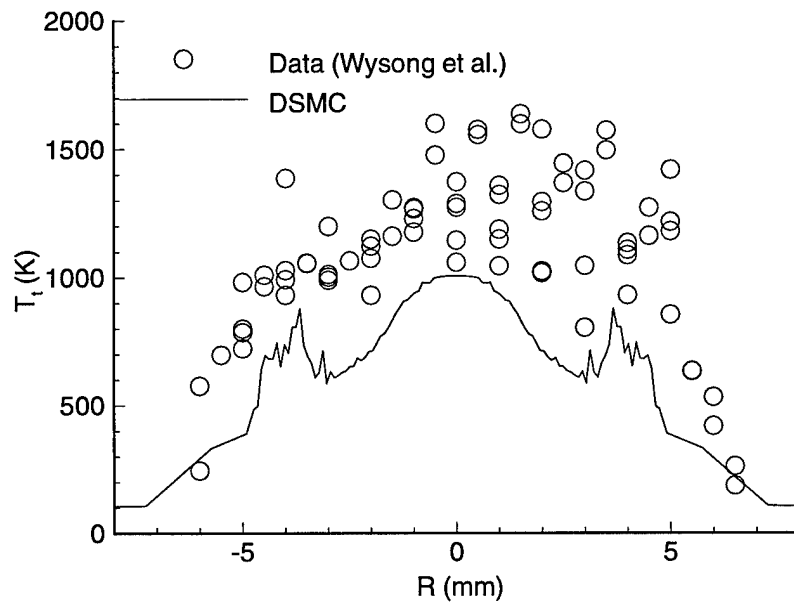


Fig. 4b. Translational temperature of atomic hydrogen in the nozzle exit plane for $P=0.80$ kW.

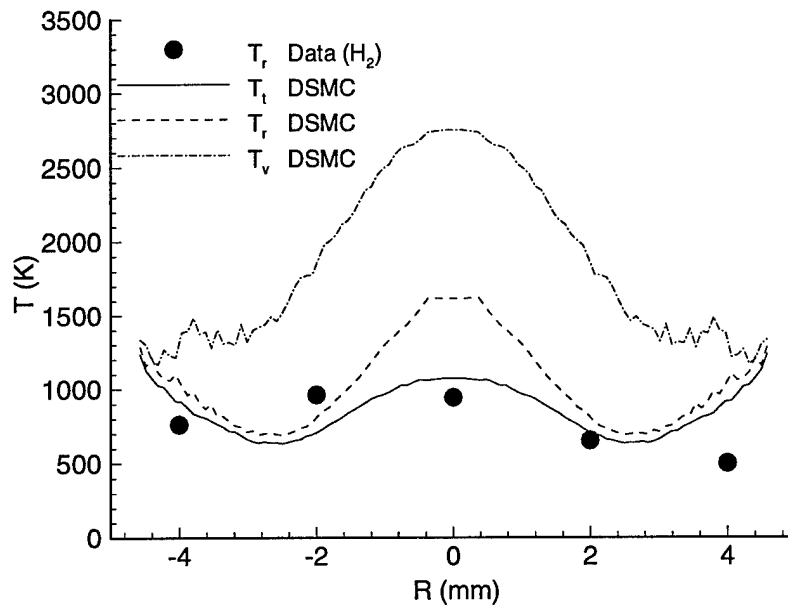


Fig. 4c. Thermal nonequilibrium of molecular hydrogen in the nozzle exit plane for $P=0.80$ kW.

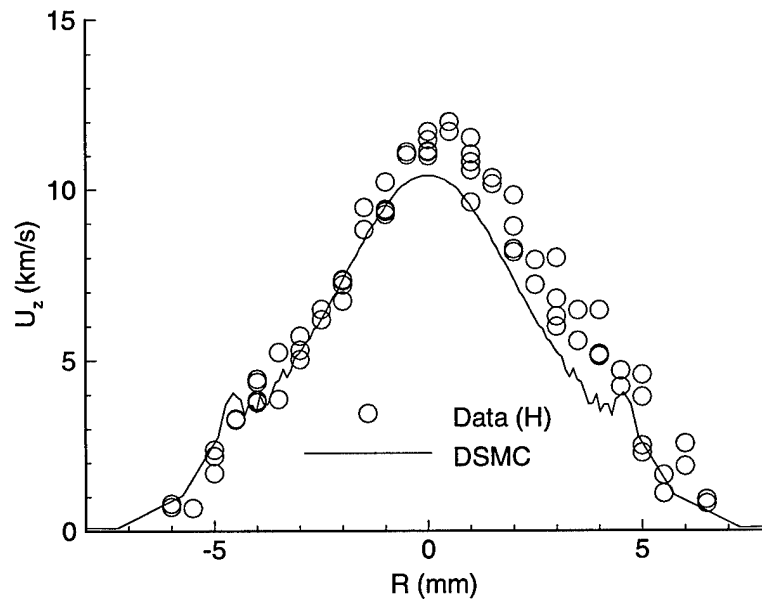


Fig. 4d. Axial velocity component of atomic hydrogen in the nozzle exit plane for $P=0.80$ kW.

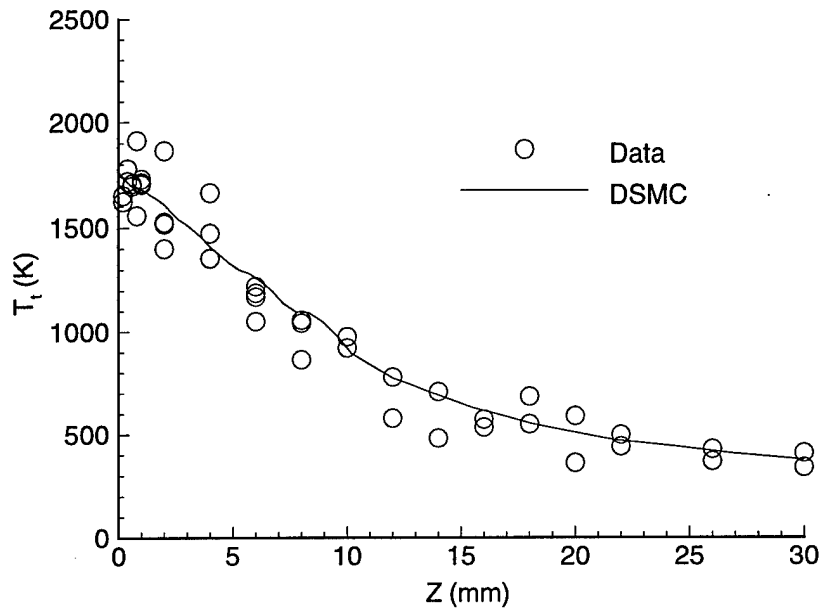


Fig. 5a. Profiles of translational temperature along the plume axis for P=1.34 kW.

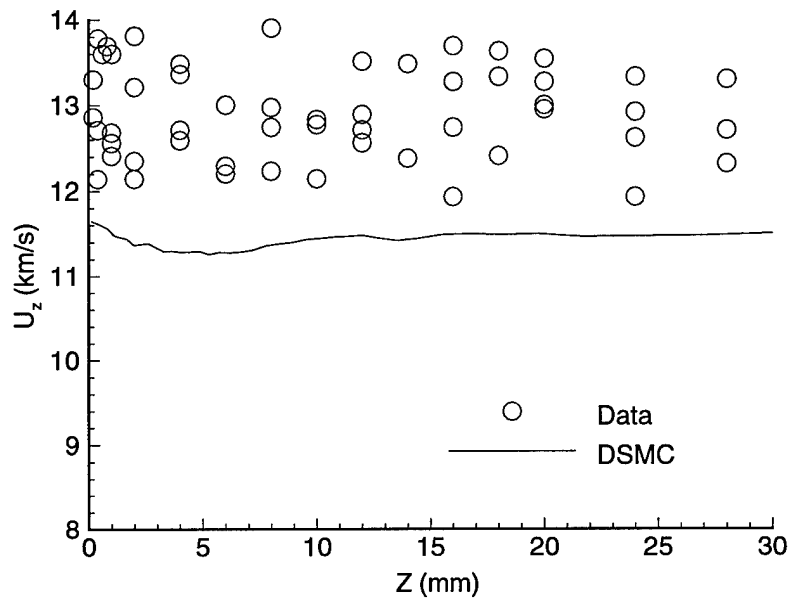


Fig. 5b. Profiles of axial velocity component along the plume axis for P=1.34 kW.

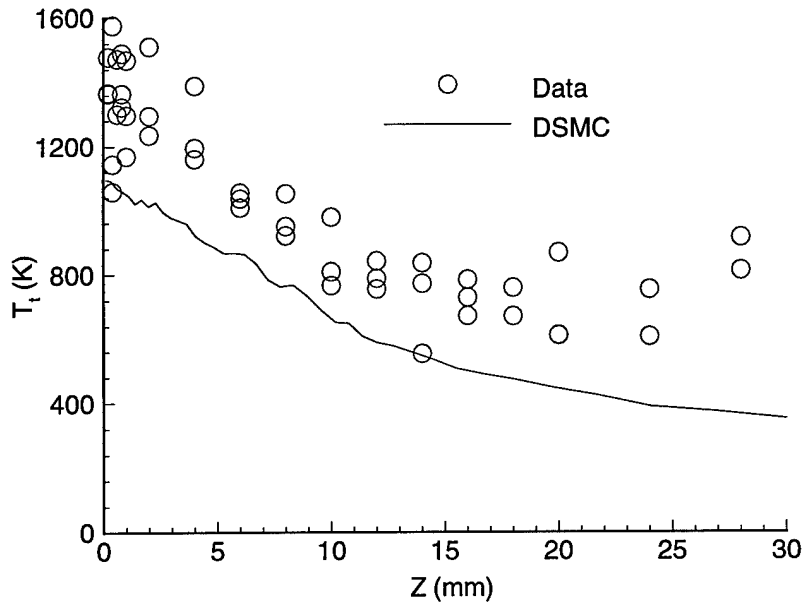


Fig. 6a. Profiles of translational temperature along the plume axis for $P=0.80$ kW.

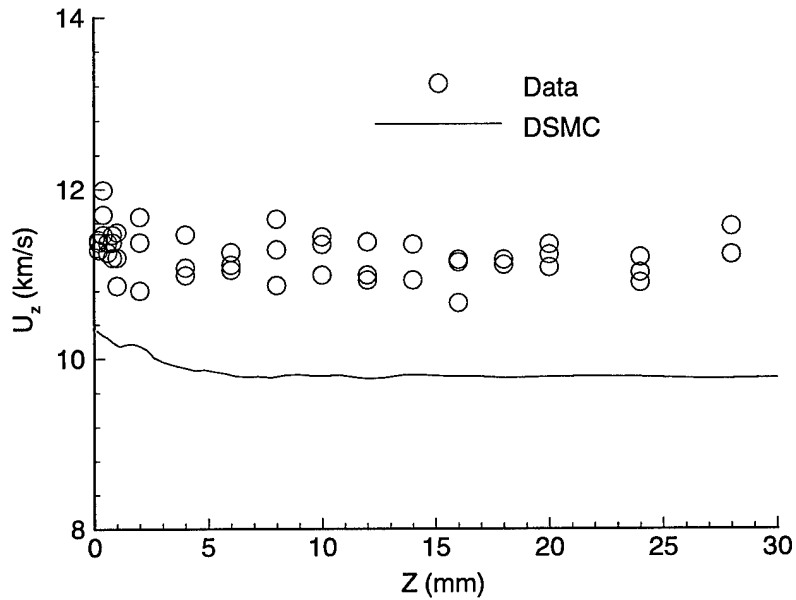


Fig. 6b. Profiles of axial velocity component along the plume axis for $P=0.80$ kW.

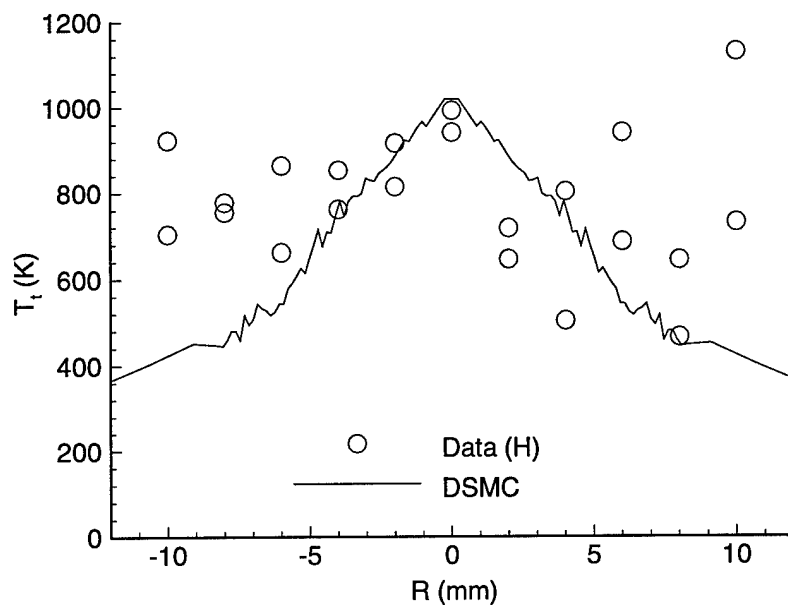


Fig. 7a. Radial profiles of translational temperature at 10 mm from the nozzle exit for $P=1.34$ kW.

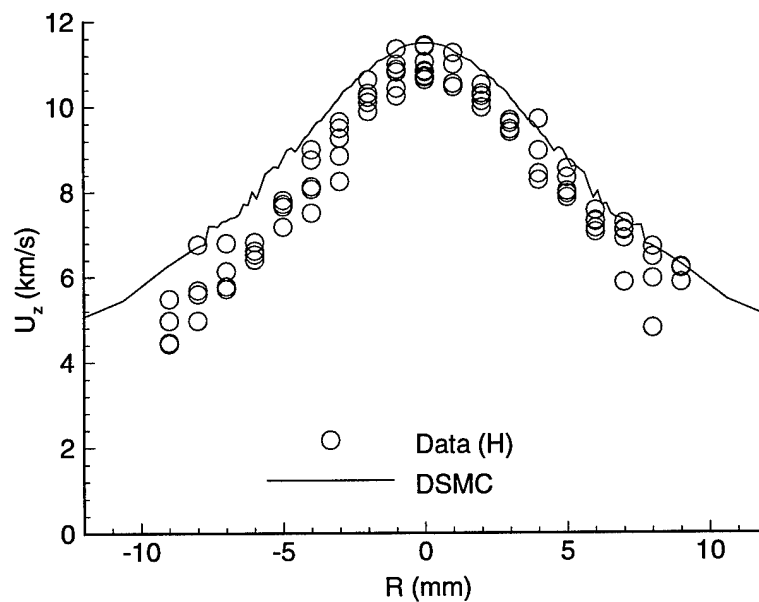


Fig. 7b. Radial profiles of axial velocity component at 10 mm from the nozzle exit for $P=1.34$ kW.

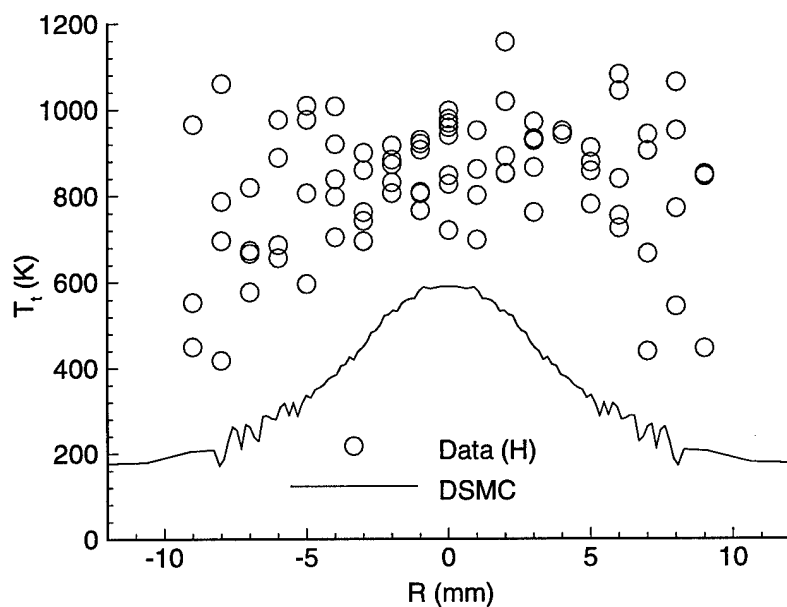


Fig. 8a. Radial profiles of translational temperature at 10 mm from the nozzle exit for $P=0.80$ kW.

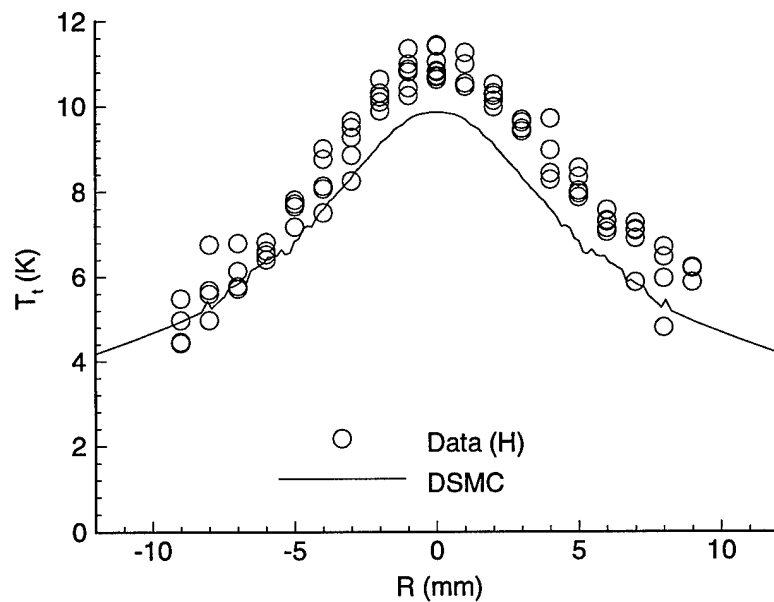


Fig. 8b. Radial profiles of axial velocity component at 10 mm from the nozzle exit for $P=0.80$ kW.

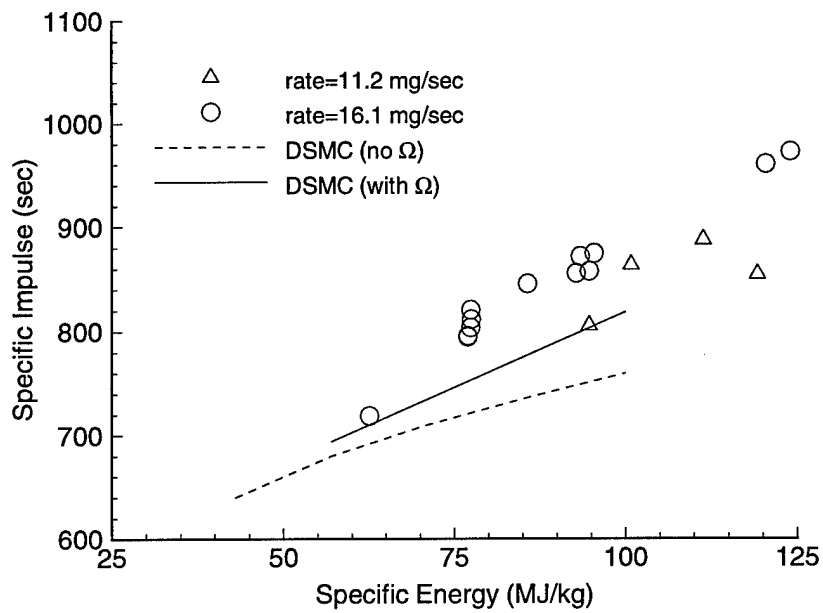


Fig. 9. Comparison of DSMC prediction and experimental measurement of specific impulse.